

## Neurons for hunger and thirst transmit a negative-valence teaching signal

**J. Nicholas Betley<sup>#</sup>, Shengjin Xu<sup>#</sup>, Zhen Fang Huang Cao<sup>#</sup>, Rong Gong, Christopher J. Magnus, Yang Yu, and Scott M. Sternson<sup>\*</sup>**

Janelia Research Campus, Howard Hughes Medical Institute, 19700 Helix Drive, Ashburn, VA 20147, USA.

<sup>#</sup> These authors contributed equally to this work.

### Abstract

Homeostasis is a biological principle for regulation of essential physiological parameters within a set range. Behavioural responses due to deviation from homeostasis are critical for survival, but motivational processes engaged by physiological need states are incompletely understood. We examined motivational characteristics and dynamics of two separate neuron populations that regulate energy and fluid homeostasis by using cell type-specific activity manipulations in mice. We found that starvation-sensitive AGRP neurons exhibit properties consistent with a negative-valence teaching signal. Mice avoided activation of AGRP neurons, indicating that AGRP neuron activity has negative valence. AGRP neuron inhibition conditioned preference for flavours and places. Correspondingly, deep-brain calcium imaging revealed that AGRP neuron activity rapidly reduced in response to food-related cues. Complementary experiments activating thirst-promoting neurons also conditioned avoidance. Therefore, these need-sensing neurons condition preference for environmental cues associated with nutrient or water ingestion, which is learned through reduction of negative-valence signals during restoration of homeostasis.

---

AGRP neurons are a hypothalamic population that is activated or inhibited by hormonal signals of energy deficit<sup>1</sup> or surfeit<sup>1</sup>, respectively. AGRP neuron ablation or inhibition suppresses feeding<sup>2,3</sup>, and activation elicits food consumption and instrumental food-seeking within minutes<sup>2,4,5</sup>, indicating that these neurons are an entry point to motivational processes resulting from homeostatic deficit<sup>6</sup>. Because food preferences and food-seeking behaviours are learned, in part, as a consequence of nutrient intake<sup>7</sup>, we investigated the capability of AGRP neurons to directly influence learning in mice.

Multiple learning processes contribute to feeding behaviour<sup>8-10</sup>. Behavioural responses to Pavlovian conditioning are typified by approach or avoidance to cues that have been

---

Reprints and permissions information is available at [www.nature.com/reprints](http://www.nature.com/reprints)

<sup>\*</sup>Correspondence to: [sternsons@janelia.hhmi.org](mailto:sternsons@janelia.hhmi.org).

#### Author Contributions

J.N.B. and S.M.S. initiated the project. J.N.B., Z.F.H.C., S.X., and S.M.S. prepared the manuscript with comments from all authors. J.N.B., S.X., Z.F.H.C., R.G., C.J.M. and S.M.S. designed the experiments and analyzed the data. J.N.B. and Z.F.H.C. performed conditioning experiments, S.X. performed *in vivo* calcium imaging experiments, R.G. and C.J.M. developed the SFO activation model for evoked water drinking, Y. Yu helped with image registration.

associated with a reinforcer<sup>8,10</sup>, such as learning preference for a nutritive food over a non-nutritive object. Instrumental conditioning is a process by which an animal learns to perform an action that elicits a valued outcome, such as lever pressing for food. Neurons that increase food-seeking and consumption in homeostatic hunger may influence these learning processes in two distinct ways. Approach to cues and performance of actions associated with food ingestion can be strengthened through the intrinsic positive valence of nutritive food<sup>7</sup>, which is potentiated during energy deficit<sup>8,11-13</sup> (Extended Data Fig 1a). Alternatively, preference or performance of actions can be conditioned by reducing states with negative valence<sup>11,14-16</sup> (Extended Data Fig. 1b). For neurons that elevate food consumption, their valence can be distinguished, in the absence of food, by whether an animal learns to prefer cues that are associated with increased or decreased activity of these neurons, respectively. Influential experiments with brain stimulation of the lateral hypothalamus found neurons that elicit food intake, have positive valence, and facilitate both Pavlovian and instrumental learning<sup>17,18</sup>. Although early behavioural theories assumed that homeostatic deficits controlled need-based behaviours by reducing a negative internal state<sup>14</sup>, neurons that increase food intake have not been reported to signal negative valence<sup>8,11</sup>.

Nevertheless, human subjects report that energy deficit is unpleasant and eating can alleviate this feeling<sup>19-21</sup>, which indicates a possible role for a poorly understood negative-valence state. Neuronal systems that elicit food-seeking and also mediate the negative valence associated with a homeostatic hunger state have not been identified. Here, we used cell type-specific neuron activity manipulations and deep-brain *in vivo* imaging to determine that hunger-promoting AGRP neurons can influence learning and behaviour through negative-valence states.

## RESULTS

### AGRP neurons condition flavour preference

To investigate whether elevated AGRP neuron activity transmits a negative-valence signal, we performed flavour preference conditioning using *ad libitum* (AL) fed mice expressing channelrhodopsin-2 (ChR2) in AGRP neurons (AGRP<sup>ChR2</sup>) (Fig. 1a-d). AGRP<sup>ChR2</sup> mice and a control AGRP<sup>EGFP</sup> group were habituated to consume two differently flavoured non-nutritive gels and were then conditioned by separately consuming one flavour during photostimulation and the other without AGRP neuron activation (Fig. 1e). After conditioning, the preference for the flavour consumed by AGRP<sup>ChR2</sup> mice during AGRP neuron photostimulation was reduced (Fig. 1f). To check whether AGRP neuron photostimulation elicits a general aversive state analogous to the nausea-inducing agent LiCl, we performed a conditioned taste aversion test by pairing a novel taste (saccharin solution) with subsequent photoactivation of AGRP neurons; there was no resulting aversion to saccharin (Extended Data Fig. 2a-c). Together, these experiments demonstrate that a flavour cue associated with high levels of AGRP neuron activity became less preferred, indicating that these neurons transmit a negative-valence signal, but AGRP neurons do not appear to elicit strong aversion or disgust, consistent with the fact that AGRP neuron activation leads to copious food consumption<sup>2,4</sup>.

AGRP neuron activity is normally elevated during energy deficit<sup>22,23</sup>. If AGRP neurons contribute to feeding behaviours through a negative-valence signal, then inhibition of AGRP neurons in food restriction was expected to facilitate learning (Extended Data Fig. 1b). For cell type-specific chemogenetic inhibition, *Agrp-IRES-Cre* mice were virally transduced to express a pharmacologically selective ligand-gated chloride channel, PSAM<sup>L141F</sup>-GlyR (AGRP<sup>PSAM-GlyR</sup> mice)<sup>24</sup> and enhanced green fluorescent protein (EGFP) (Fig. 1g-i, Extended Data Fig. 2d). As previously characterised<sup>24</sup>, intraperitoneal (i.p.) administration of the channel's cognate selective synthetic ligand (PSEM<sup>89S</sup>) inhibited AGRP neuron activity (Extended Data Fig. 2e-g), and reduced food consumption (Fig. 1j, Extended Data Fig. 2h) to an extent that correlated with the transgene transduction efficiency (Extended Data Fig. 2i-n). We measured flavour preference associated with AGRP neuron silencing in food-restricted (FR) AGRP<sup>PSAM-GlyR</sup> mice (85-90% body weight). Preference increased for the flavour consumed during AGRP neuron inhibition (Fig. 1k), and the change in flavour preference correlated with reduction of chow re-feeding by AGRP neuron silencing (Fig. 1l,m). Therefore, inhibiting AGRP neuron activity in energy deficit conditions flavour preference, consistent with suppression of a negative-valence signal.

### AGRP neurons condition place preference

We also examined whether AGRP neurons influenced preference for contextual cues independently of ingestive behaviours. First, we performed place preference conditioning by inhibiting AGRP neurons in the absence of food (Fig. 2a). Using a two-sided chamber, FR, but not AL-fed, AGRP<sup>PSAM-GlyR</sup> mice increased occupancy time in the chamber paired with PSEM<sup>89S</sup>, while control AGRP<sup>EGFP</sup> FR mice did not shift place preference (Fig. 2a-c). The extent of the shift in occupancy time for FR mice positively correlated with the transduction efficiency of the PSAM<sup>L141F</sup>-GlyR-*IRES*-EGFP transgene (Fig. 2d) as well as a *post hoc* food intake reduction test during AGRP neuron silencing (Fig. 2e). Furthermore, for a subset of mice that were subjected sequentially to both conditioned place preference and flavour preference tests with AGRP neuron silencing, the magnitude of the preference shift was correlated between the two conditioning assays (Fig. 2f). This demonstrates a conditioning process where reduction of electrical activity in this neuron population during energy deficit reduces food intake and also increases preference for associated contextual and flavour cues.

We next investigated whether the negative-valence properties of AGRP neuron activation influenced conditioned place preference. While passive conditioning to AGRP neuron stimulation was neither sufficient to reliably change place preference<sup>25</sup> (Occupancy time:  $28.4 \pm 72$  s;  $p=0.70$  paired t-test,  $n=10$ ) nor to oppose cocaine conditioned place preference (Preference, AGRP<sup>EGFP</sup>/coc:  $25.2 \pm 4.2\%$ ,  $n=6$ ; AGRP<sup>ChR2</sup>/coc:  $32.7 \pm 8.6\%$ ,  $n=6$ ;  $p=0.45$ ), we sought to determine if the contrast between high and low AGRP neuron activity was learned more effectively. Following passive conditioning, mice were tested each day while freely exploring the conditioning apparatus, and AGRP neuron photostimulation was triggered whenever the mouse entered the side previously exposed to photostimulation (Methods and Fig. 2g). Over the course of multiple sessions, mice showed avoidance of the side paired with AGRP neuron photostimulation (Fig. 2h,i). This effect was more robust for the second half of the closed-loop place preference session (Fig. 2j), which is likely related

to the previously reported minutes-long latency of AGRP neuron stimulation to evoke feeding<sup>4</sup>. In a subsequent extinction test in the absence of photostimulation, mice preferred the side that had been associated with cessation of AGRP neuron photostimulation (Fig. 2k and Extended Data Fig. 3a,b). These experiments further indicate that AGRP neurons transmit a negative-valence signal, and discontinuing AGRP neuron photostimulation can condition preference for contextual cues.

The temporal properties and the magnitude of the response to passive place conditioning indicate that AGRP neuron activation is not a strongly aversive stimulus, such as a shock<sup>16</sup>, that is capable of eliciting goal-directed instrumental avoidance responses. Indeed, attempts to condition mice to perform an instrumental action (lever-press or nose-poke) to either shut off AGRP neuron photostimulation in well-fed mice or to optogenetically silence AGRP neurons in food-restricted mice were unsuccessful (see Methods and Extended Data Fig. 3c-i). Therefore, these experiments indicate that AGRP neuron activity is associated with a negative-valence signal that can mediate Pavlovian learning, but this property does not readily extend to instrumental conditioning.

### Modulation of instrumental food-seeking

Although manipulation of AGRP neuron activity does not appear to directly reinforce instrumental responses, AGRP neuron activation leads to vigorous performance of previously learned instrumental food-seeking responses<sup>2,5</sup>. We examined whether AGRP neuron-evoked instrumental responding for food may be sensitive to the negative valence of these neurons. If AGRP neuron activity influences food-seeking behaviours through a negative-valence signal (Extended Data Fig. 1b), then previously reinforced lever-pressing actions would gradually decrease during AGRP neuron photostimulation because nutrient ingestion would not be capable of reducing exogenously elevated AGRP neuron activity. As an alternative hypothesis, if AGRP neuron activity predominantly influenced food-seeking by enhancing the positive valence of food consumption (Extended Data Fig. 1a), then lever-pressing would remain elevated.

We initially compared two groups of mice that were trained to lever-press on a progressive ratio-7 (PR7) food reinforcement schedule under food restriction (Fig. 3a). After learning the contingency between lever-pressing and food delivery, one group that was maintained under food restriction showed steady lever-press responses for 15 sessions. The other group was re-fed *ad libitum* and was tested for instrumental food-seeking during AGRP neuron photostimulation, where AGRP neuron stimulation was continued after the levers and food access were withdrawn (Fig 3a). AL-fed mice initially responded to AGRP neuron photostimulation with high lever-press rate and food consumption, similar to FR-mice (t-test,  $p=0.491$ ; Fig. 3b). In subsequent sessions, photostimulated AL-fed AGRP<sup>ChR2</sup> mice showed a progressive decline in lever-presses, pellets consumed, and break point (Fig. 3c-e and Extended Data Fig. 4a-c). Lever-pressing was reduced nearly to the low levels observed without photostimulation (Fig. 3b and Extended Data 4a-c), and pressing at high-effort response ratios was most strongly diminished (Fig. 3f,g). In a separate group, using a shorter photostimulation protocol, lever-pressing was reduced to an intermediate level (Extended Data Fig. 4d-f). We noted an increase in body weight during the multi-session AGRP neuron

stimulation protocol, but suppression of lever pressing for food was not due to these long-term metabolic changes (Extended Data Fig. 5). Furthermore, *ad libitum* food intake during AGRP neuron photostimulation was not altered with the extended stimulation protocol, indicating that reduced instrumental food-seeking was not due to food aversion or diminished effectiveness of repeated AGRP neuron photostimulation (Extended Data Fig. 6). Taken together, progressive reduction of AGRP neuron-evoked instrumental food-seeking responses in AL-mice is consistent with the negative-valence properties of AGRP neurons and indicates reduced value of nutritive food when AGRP neuron activity remains elevated.

### Food rapidly inhibit AGRP neurons

AGRP neuron electrical activity manipulations condition learning, but an essential consideration is the correspondence of perturbation studies to the endogenous activity patterns of AGRP neurons during feeding behaviours. To investigate this, we monitored AGRP neuron activity in freely moving mice using deep-brain imaging of genetically encoded calcium indicators through an intracranial gradient index (GRIN) lens with a head-mounted miniature microscope<sup>26</sup> (Fig. 4a,b).

Genetically encoded calcium indicators (GCaMP6f or GCaMP6s<sup>27</sup>) were expressed in AGRP neurons (Fig. 4c,d) and were well tolerated (Extended Data Fig. 7a). Characterization in brain slices revealed sharp increases in calcium activity during burst firing, while changes in tonic firing were detected as a gradual change in the baseline fluorescence (Extended Data Fig. 7b). Characterization *in vivo* by injection of the orexigenic hormone ghrelin substantially increased GCaMP6 brightness and dynamic responses in 81% of AGRP neurons (Extended Data Fig. 7c-e, Supplementary Video 1, 4% of AGRP neurons decreased), which subsequently returned to baseline levels (population  $t_{1/2}$ : 19 min, individual neuron  $t_{1/2}$  range: 5-46 min, Extended Data Fig. 7f,g). Therefore, imaging AGRP neuron calcium dynamics allows individual neuron activity patterns to be monitored *in vivo*, and these responses are consistent with previously reported electrical activity changes *ex vivo*<sup>1</sup>.

We used deep-brain calcium imaging to monitor AGRP neuron activity in FR mice, which was elevated over the AL-fed condition in 54/61 AGRP neurons (Fig. 4e). Delivery of a mouse chow pellet to FR mice resulted in rapid reduction of GCaMP6 fluorescence during food consumption in 106/110 neurons (96%, 4 mice, Fig. 4f-I, Supplementary Video 2); 1/110 neurons increased fluorescence. Removal of the food, after less than 50 mg had been consumed, was followed by a gradual increase in AGRP neuron calcium activity to a level that remained slightly below the initial baseline value (Fig. 4j). In contrast, a false-food pellet (e.g., wood block) only transiently reduced AGRP neuron activity, which rapidly recovered after the mouse contacted the object (Fig 4g,h). Subsequent trials with short exposure to food led to progressive decline in baseline fluorescence that was significantly larger than for the false-food object (Fig. 4j and Extended Data Fig. 7h). These experiments show that, in FR mice, baseline AGRP neuron activity was gradually reduced by the consumption of nutritive food, in line with homeostatic regulation, but AGRP neuron

activity was also rapidly and strongly suppressed during initiation of food consummatory behaviours.

Further analysis of the rapid response to nutritive chow food pellets revealed that calcium activity was reduced prior to food consumption (Fig. 4k). Moreover, presentation of a visible but inaccessible food pellet, reduced AGRP neuron activity nearly to the same level as during a subsequent food consumption trial (Extended Data Fig. 7i, Supplementary Video 3). These observations demonstrate that AGRP neuron activity is inhibited by food-related cues before nutrients are tasted or consumed. To examine if this rapid AGRP neuron inhibition involves learning, we used Pavlovian trace conditioning to determine the capability of an initially neutral conditioned stimulus (CS) to control AGRP neuron activity. Initial exposure to a 200 ms auditory and visual compound CS showed a slight increase of mean AGRP neuron calcium activity (Fig. 4l), but consumption of a palatable liquid food delivered by presentation of a lick spout reduced AGRP neuron GCaMP6 fluorescence. After repeatedly pairing the CS with food presentation, the CS elicited reduction of AGRP neuron activity (prior to spout extension,  $p < 0.001$ , unpaired t-test), and food consumption had little additional effect (Fig. 4l). Therefore, AGRP neurons predictively encode the receipt of nutritive food by rapidly reducing activity, and this process involves learning. Together with neuron silencing and activation experiments (Figs. 1-3), these studies demonstrate that endogenous AGRP neuron dynamics during eating correspond to the activity manipulations that conditioned preference for flavour and contextual cues. Moreover, the rapid recovery of AGRP neuron activity during false food exposure is expected to reduce preference for non-food objects because AGRP neuron activity signals negative valence.

### A virtual thirst state is avoided

Is a negative-valence signal used by other homeostatic neurons that mediate a different survival need? To investigate this, we developed an animal model of evoked-thirst by chemogenetic and optogenetic induction of water-seeking and consumption. Prior work has shown the importance of the subfornical organ (SFO) in the brain for mediating water intake<sup>28,29</sup>. Chemogenetic SFO activation selectively elevated consumption of water, but not food, and increased breakpoint for water on a progressive ratio-3 schedule (Extended Data Fig. 8a-i). Elevated drinking was observed by optogenetically activating a SFO neuron subpopulation molecularly defined by expression of *nitric oxide synthase 1* (*Nos1*) (Fig. 5a-c'). SFO<sup>NOS1-ChR2</sup> photostimulation rapidly increased water consumption (latency, 20 Hz:  $3.8 \pm 0.5$  minutes,  $n=8$ ) at a range of photostimulation frequencies (Fig. 5d) but not food intake (Extended Data Fig. 8j).

To examine the conditioning properties of SFO<sup>NOS1</sup> neurons, we used the same closed-loop place conditioning protocol as for AGRP neurons (see Fig. 2g). Over the course of 7 sessions, mice showed avoidance of the side paired with SFO<sup>NOS1</sup> neuron photostimulation (Fig. 5e-f'). In a subsequent extinction test in the absence of photostimulation, mice preferred the side associated with cessation of SFO<sup>NOS1</sup> neuron photostimulation (Fig. 5g). These experiments show that places associated with SFO<sup>NOS1</sup> neuron activation are

avoided, which demonstrates a negative-valence signal that can condition learning from a second homeostatic neuronal cell type with a distinct biological function.

## DISCUSSION

Physiological need states, in part acting through circulating hormones, lead to elevated electrical activity of specialized need-sensitive neurons, such as AGRP and SFO<sup>NOS1</sup> neurons. Here, we show that these molecularly defined neuron populations signal negative valence. Through the reduction of negative-valence signals, preference for cues associated with lessening of physiological need states can be learned.

Correspondingly, deep-brain calcium imaging demonstrated that AGRP neuron activity is rapidly inhibited during both food consumption and by cues that predict food. Recent measurement of mean population activity in AGRP neurons also found fast inhibitory dynamics<sup>30</sup>, and we show that nearly all AGRP neurons have this property. We also find that rapid reduction of AGRP neuron activity involves the learned association of sensory information with food consumption, highlighting the existence of neural circuit inputs carrying information about conditioned stimuli. Moreover, sustained reduction of AGRP neuron activity requires nutrient ingestion, consistent with homeostatic regulation, likely involving well-established hormonal control mechanisms.

The valence of increased AGRP neuron activity is opposite to analogous neuronal perturbations in the lateral hypothalamus, which also lead to avid food consumption but exhibit rewarding properties<sup>17,18,31,32</sup>. This may reflect mechanistic differences between homeostatic and hedonic motivation for food, which, for the latter, is primarily distinguished by appetite for highly palatable food even in the absence of a need state<sup>33</sup>. Our experiments, taken together with other studies, indicate that homeostatic need states regulate behaviour through a combination of negative and positive valence signals contributing to Pavlovian and instrumental conditioning. Modulation of both processes can be coordinated by hormones such as ghrelin, leptin, and angiotensin<sup>34-36</sup> as well as synaptic inputs<sup>37,38</sup>. Under homeostatic deficit, negative and positive reinforcement processes are expected to operate in a concerted push-pull manner, respectively, to achieve outcomes that have the highest value in that state.

The negative valence of elevated AGRP and SFO<sup>NOS1</sup> neuron activity is also consistent with human self-reports of negative feelings associated with hunger and thirst arising from homeostatic deficits<sup>20,39</sup>. The behavioural characteristics of AGRP neuron activity in mice parallel some negative emotional aspects of weight loss in humans, which contribute to low long-term behavioural compliance on weight-loss diets<sup>19,21</sup>. The failure to maintain weight-loss reverses its multifaceted clinical benefits, such as lessening diabetes and hypertension symptoms. Our experiments show that AGRP neuron circuits, which are conserved in humans, provide an entry point to investigate the relationship between metabolism and negative emotional states.

## METHODS

All experimental protocols were conducted according to U.S. National Institutes of Health guidelines for animal research and approved by the Institutional Animal Care and Use Committee at Janelia Farm Research Campus.

### Mice

Mice were housed on a 06:00-18:00h light cycle with water and mouse chow *ad libitum* (PicoLab Rodent Diet 20, 5053 tablet, TestDiet) unless otherwise noted. Adult male mice (>8 weeks) were used for experiments. Cre recombinase-expressing lines were used: *Agrp-IRES-Cre* (Jackson Labs Stock 012899, *Agrp<sup>tm1(cre)Lowl/J</sup>*), *Nos1-IRES-Cre* (Jackson Labs Stock 017526, B6.129-*Nos1<sup>tm1(cre)Mgmj/J</sup>*). For channelrhodopsin-2 expression in AGRP neurons, *Agrp-IRES-Cre* mice were crossed with *Ai32: ROSA26-loxStoplox-ChR2-EYFP* (Jackson Labs stock 012569, B6;129S-*Gt(ROSA)26Sor<sup>tm32(CAG-COP4\*H134R/EYFP)Hze/J</sup>*). For EGFP in AGRP neurons, *Agrp-IRES-Cre* mice were crossed with ROSA-GNZ: *ROSA26-loxStoplox-GFP-NLS-LacZ* (Jackson Labs stock 008516). For Arch in AGRP neurons, *Agrp-IRES-Cre* mice were crossed with *Ai35d: ROSA-CAG-loxStoplox-Arch-GFP-WPRE* (Jackson Labs stock 012735). C57BL/6J mice were from Jackson Labs (stock 000664).

### Recombinant adeno-associated viral (rAAV) vectors

The following Cre-dependent viral vectors<sup>40,41</sup> were used in this study: rAAV2/10-CAG-FLEX-*rev*-ChR2tdtomato (3e13 Genomic Copies (GC)/ml, University of Pennsylvania vector core), rAAV2/1 and rAAV2/9-*hSyn*-FLEX-*rev*-PSAM<sup>L141F</sup>-GlyR-*IRES*-EGFP (1.4e13 and 1.5e13 GC/ml, respectively, Janelia, [http://www.addgene.org/Scott\\_Sternson/](http://www.addgene.org/Scott_Sternson/)), rAAV2/9-CAG-FLEX-EGFP (7e12 GC/ml, Penn), rAAV2/1-*hSyn*-Cre (5.6e12 GC/ml, Janelia), rAAV2/2-*Efl1a*-DIO-hChR2(H134R)-EYFP (6e12 GC/ml, UNC vector core), rAAV2/2-*Efl1a*-DIO-hM3D(Gq)-mCherry (3e12 GC/ml, UNC), AAV2/1-*Syn*-FLEX-GCaMP6f and AAV2/1-*Syn*-FLEX-GCaMP6s (10<sup>12</sup> to 10<sup>13</sup> GC/ml, Janelia). CAG: promoter containing: a cytomegalovirus enhancer; the promoter, first exon, and first intron of the chicken beta actin gene; and the splice acceptor of rabbit beta-globin gene. *Efl1a*: Human elongation factor-1 alpha promoter. FLEX: Cre-dependent flip-excision switch. DIO: double-floxed inverted orientation.

### Viral injections and optical fibre placement

Viral injections and implantation of ferrule-capped optical fibres (200 µm diameter core, multimode, NA 0.48, ThorLabs) were performed as described previously<sup>23</sup>. Bilateral ARC viral injections in *Agrp-IRES-Cre* mice were made at two depths using the following coordinates: bregma: -1.3 mm; midline: ±0.3 mm; dorsal surface: -5.95 mm and -5.85 mm (250-500 nl/site). Bilateral SFO viral injections were made at bregma: -0.35 mm, midline: ±0.6 mm, dorsal surface: -2.45 mm (100-300 nl/site).

After 2-4 weeks for transgene expression, a ferrule-capped optical fibre was placed: for AGRP<sup>ChR2</sup> mice over the ARC (bregma -1.4 mm, midline: +0.25 mm, dorsal surface 5.6 mm); for SFO<sup>Nos1-ChR2</sup> mice over the SFO (bregma: -0.35 mm, midline: ±0.6 mm, dorsal surface: -2.3 mm, approach angle: 12°).



## Immunohistochemistry

Immunohistochemistry was as described previously<sup>23</sup>. Antibodies: goat anti-AGRP (1:5000, Neuromics, GT15023), guinea pig anti-RFP (1:25000, Covance), rabbit anti-Fos (1:5000, Santa Cruz, SC-52, Lot-C1010), rabbit anti-GFP (1:5000, Invitrogen, A-11122). Confocal images (Zeiss LSM 510 microscope) were acquired first from Fos-immunostained tissue taken from a food deprived mouse, as described previously<sup>23</sup>. These image acquisition settings were maintained for all quantitative Fos analysis (each condition: >50 nuclei from 3 mice, selected blind to the Fos-immunofluorescence levels). Transgene transduction efficiency in AGRP neurons was determined as previously described<sup>23</sup> (from >500 AGRP boutons, multiple sections).

## Food restriction

Food intake was adjusted to maintain mice at 85-90% of their initial AL-fed body weight, and food was consumed 18-h before subsequent behavioural assays.

## AGRP neuron inhibition *in vivo*

For AGRP neuron silencing, mice expressing PSAM<sup>L141F</sup>-GlyR in AGRP neurons (AGRP<sup>PSAM-GlyR</sup> mice) were injected intraperitoneally (i.p.) with the ligand PSEM<sup>89S</sup> (30 mg/kg) dissolved in saline.

**Suppression of refeeding in food-restricted mice**—In food-restricted AGRP<sup>PSAM-GlyR</sup> mice two 1-h food intake measurements were performed early in the light period and separated by a day. Saline or PSEM<sup>89S</sup> (30 mg/kg) were administered 30 minutes before food was provided, at the time food was provided, and 30 minutes later (multiple administration of PSEM<sup>89S</sup> was used due to its rapid clearance<sup>24</sup>).

**Suppression of Fos expression by AGRP Neuron Silencing**—In AL-fed mice, Fos immunofluorescence intensity was measured in AGRP neurons from AGRP<sup>PSAM-GlyR</sup> (n=3) and AGRP<sup>EGFP</sup> (n=3) during the dark period after PSEM<sup>89S</sup> treatment (30 mg/kg). Fos expression in AGRP neurons is elevated in the dark period in the absence of food, which was removed from the mice at the beginning of the dark period (18:00). PSEM<sup>89S</sup> (30 mg/kg) was injected 30 min before the onset of the dark period and subsequently every 45 minutes for 5 hours (injection frequency is due to pharmacokinetics of PSEM<sup>89S</sup>)<sup>24</sup>. Mice were deeply anesthetized and then perfused, and the brain was dissected for immunohistochemical analysis.

**Suppression of Dark Period Feeding**—AL-fed mice were injected with either saline (test day 1) or PSEM<sup>89S</sup> (test day 2). At the onset of the dark period, mice were injected again and given free access to chow. PSEM<sup>89S</sup> (30 mg/kg) or saline was administered every hour until the assay concluded at 22:00; food consumption was recorded.

## Photostimulation *in vivo*

Photostimulation was as described previously<sup>23</sup>. Light pulse protocol: 10 ms pulses, 20 Hz (unless otherwise noted) for 1 s, repeated every 4 seconds.

### Conditioned Flavour Preference

Food-restricted AGRP<sup>PSAM-GlyR</sup> mice and AGRP<sup>EGFP</sup> control mice were acclimatized for four sessions (15 min) to consumption of two non-nutritive gels that were sweetened with sucralose but differed by flavour (orange and strawberry). Prepackaged Hunts® sugar free Juicy Gels were used that contained 0.05 kcal/g (for comparison, 4.1 kcal/g in chow). Consumption during last two sessions was used to determine initial flavour preference (no significant initial group flavour preference,  $p=0.41$ , t-test). For flavour preference conditioning, mice were given two daily 30-min sessions (repeated over 4 days) with each gel individually, separated by 4 hours, with the order of conditioning for the gels inverted each day. The initially preferred flavoured gel was presented paired with saline injection, and the less preferred flavoured gel was paired with injection of PSEM<sup>89S</sup> (30 mg/kg) (each injection after 5 min of consumption). After conditioning, equal quantities of the two gels were presented (15 min) and the amount of each flavour consumed was recorded. This was repeated the following day with the position of the gel inverted and preferences from the two test sessions were averaged.

To examine conditioned flavour preference learning during AGRP neuron activation, AGRP<sup>ChR2</sup> mice and AGRP<sup>EGFP</sup> control mice implanted with a ferrule-capped optical fibre over the ARC were used. Mice were conditioned as above with photostimulation, with the following differences. AL-fed mice were used and were acclimatized to consume the two non-nutritive overnight (3 g). For conditioning, in one session, the mouse was presented with 0.3 g of its preferred flavoured gel, and after 5 minutes, intracranial light pulses were applied for an additional 25 minutes. In the other session, the mouse was presented with 0.3 g of the less preferred flavoured gel, and the mouse was kept in the cage for 30 minutes without any light applied to the fibre. Mice typically ate the entire 0.3 g during each session. After conditioning, the AL-fed mice were presented again with equal quantities of the two gels for two 15 minute test sessions as described above.

### Conditioned Taste Aversion

AGRP<sup>ChR2</sup> mice with implanted ferrule-capped optical fibres were used for all groups (LiCl, Saline, Photostimulation, No Photostimulation; all  $n=6$  mice). Mice were placed on water-restriction. After acclimation to sipper tubes, the four groups were allowed to consume a tastant (0.15% saccharine solution, 20 min), and the amount was recorded. For LiCl and Saline groups, mice were injected with either LiCl (125 mg/kg) or saline (0.9%) immediately following the exposure to the tastant. After 48 h, consumption of tastant was tested (20 min). On the next day, consumption of water (20 min) was measured. For the Photostimulation group, mice received AGRP neuron photostimulation for 120-min immediately following exposure to tastant. The No photostimulation group was tethered with a fibre for the same period of time, but no light pulses were delivered. On the next day, consumption of tastant solution (20 min) was measured, followed by further photostimulation conditioning (total: 4 conditioning and 4 test sessions). The day after the last test session (Test 4), consumption of water (20 min) was measured.

## Conditioned Place Preference

A two chambered apparatus was used with visual (black and white sides) and textural cues (black side: plastic grid (3mm holes) flooring, white side: soft textured side of Kimtech bench-top-protector #7546 Kimberly-Clark). The floor was back-lit (luminance ~100 Lux), and an overhead video camera recorded position (Basler, 3.75 Hz frame rate, gVision software, <http://gvision-hhmi.sourceforge.net/>). The apparatus was in a sound isolation chamber. AL-fed AGRP<sup>PSAM-GlyR</sup> mice and AGRP<sup>EGFP</sup> controls were acclimatized (15 min). The following day, the mouse's position was recorded (1800 s) and tracked offline using Ctrax<sup>42</sup>, and the initial side preference was determined. Mice were then food restricted (FR) to 85-90% of their initial body weight before conditioning sessions. Daily conditioning consisted of two 1800-s sessions: 1) the initially preferred side of the chamber paired with saline injection; 2) the initially less preferred side paired with PSEM<sup>89S</sup> (30 mg/kg) injection. After five conditioning days, mice were AL re-fed. The following day, mice were given free access to the entire apparatus and their position was tracked. The change in occupancy is the change in time spent on the initially less preferred side following training, for which positive numbers reflect increased preference for the side on which they were injected with PSEM<sup>89S</sup>. An additional set of AGRP<sup>PSAM-GlyR</sup> mice was tested on the above protocol with the following modification: before the daily conditioning sessions, mice were given free access to mouse chow for 2.5 hours, during which time they consumed 2–3 g.

## Closed-loop place preference

Conditioning for AGRP<sup>ChR2</sup> optogenetic neuron photostimulation was performed with a two step protocol alternating passive conditioning with a closed-loop place preference test. The closed-loop place preference protocol alone was less reliable for conditioning avoidance, likely related to the minutes-long latency<sup>4</sup> of AGRP neuron activation to induce food-seeking and consumption. Therefore, some prior experience with prolonged AGRP neuron activity on one of the sides appears to improve efficacy, although this exposure alone did not significantly alter place preference. Passive conditioning sessions involved separate exposure to each side of the apparatus (1800 s each) with the mouse tethered to the fibre, where the initially more preferred side was paired with intracranial light pulses to photostimulate AGRP neurons. Passive conditioning was followed by closed-loop place preference testing on the subsequent day, in which mice were allowed free access to both sides of the chamber and photostimulation was applied when the mouse entered the side of the chamber also paired with photostimulation during passive conditioning (photostimulation ceased as soon as the mouse crossed to the other side). After 7 conditioning-days (morning: closed- loop place preference, afternoon: passive conditioning), the mice were given free access to the chamber for 1800-s without photostimulation (extinction test). AGRP<sup>EGFP</sup> control mice were treated identically. The same protocol was used for conditioning SFO<sup>NOS1-ChR2</sup> mice (Fig. 5).

## Cocaine place preference

Conditioning for AGRP<sup>ChR2</sup> or AGRP<sup>EGFP</sup> optogenetic neuron photostimulation was performed in combination with a cocaine injection. Three passive conditioning sessions involved separate exposure to each side of the apparatus (1800-s each) where the initially

less preferred side was paired with intracranial light pulses and i.p. cocaine administration (10 mg/kg), and the initially preferred side was paired with saline injection and no photostimulation.

### **Post hoc assessment of conditioned appetite**

After conditioning avoidance of the side associated with AGRP neuron activation, AGRP<sup>ChR2</sup> mice were subsequently tested for the possibility that AGRP neuron activation might have conditioned elevated appetite in the context associated with prior AGRP neuron activation. *Ad libitum* fed mice in the light period (09:00-12:00) were restricted to the side of the chamber previously associated with photostimulation in which they were given free access to food for 1 hour. In a subsequent session performed on a different day, the mouse was confined to the other side of the chamber and also given free access to food for 1 hour. The side order was counterbalanced, and exposure to food on both sides was in the absence of photostimulation.

### **Instrumental conditioning**

Training and tests were conducted in operant conditioning chambers (Coulbourn Instruments) housed in sound isolation chambers as previously described<sup>23</sup>.

**Negative reinforcement**—Male AGRP<sup>ChR2</sup> mice implanted with a ferrule-capped optical fibre over the ARC were used if they consumed at least 0.7 g of food (20 mg grain pellets, TestDiet) during photostimulation as a test for proper fibre placement. We adapted a negative reinforcement instrumental conditioning protocol that was previously established for avoidance of optogenetic lateral habenula photostimulation<sup>43</sup>. Conditioning chambers had two nose poke ports, both with backlighting: one active port to stop AGRP neuron photostimulation and one inactive. AGRP<sup>ChR2</sup> mice were photostimulated and each nose poke resulted in 20-s pause for light pulses, and a tone and houselight cue were turned on until the laser stimulation returned (session time: 20 min).

A different set of male AL-fed AGRP<sup>ChR2</sup> mice were first trained to perform a lever pressing task on a fixed ratio schedule (FR1) in order to obtain food. Training occurred overnight, and a minimum of 50 lever presses was the inclusion criterion. The protocol above was applied where photostimulation pause was contingent on lever pressing.

Instrumental conditioning for AGRP neuron inhibition. AGRP<sup>Arch</sup> mice (*Agrp-IRES-Cre;Ai35d*) were food restricted to 85-90% of their bodyweight. Testing was in sound isolation boxes with operant chambers containing one backlit nose poke port. Each nose poke resulted in 60 s of light (561nm) delivery at a power of 15 mW delivered from fibre tip, in conjunction with onset of tone and houselight cues (session length: 1 h). AGRP neurons were estimated to receive irradiance of >15 mW/mm<sup>2</sup> (<http://www.openoptogenetics.org>).

### **Progressive ratio-7 food reinforcement schedule**

Male AGRP<sup>ChR2</sup> mice implanted with a ferrule-capped optical fibre over the ARC were used for instrumental conditioning in a lever-press task for food. Mice were used that

consumed at least 0.7 g of food during a 1-h photostimulation test. Mice that did not reach this criterion were used for the control (food restricted) group.

Experiments were conducted in operant conditioning chambers with two retractable levers, one active (delivered food pellets) and one inactive (did not deliver food pellets), at either side of the food hopper, and chambers were housed in sound isolation boxes. Levers were extended at the start of each session. After reaching lever-press criteria for a reward, levers were retracted and a food pellet was delivered. Five seconds after pellet removal from the food hopper, levers were extended again.

**Training**—Food rewards during training consisted of grain pellets (20 mg) with identical composition to homecage food. Lever-press training was conducted under food restriction, where mice were maintained at ~85% body weight. All mice were trained to lever press for food with a FR1 reinforcement schedule overnight for one night. Mice were trained on daily, 30-minute FR1 sessions until reaching learning criteria (earning 18 pellets in a 30-minute session for 3 consecutive days). They were then trained with 2-hour sessions for two days on a progressive ratio schedule where the required number of presses for each subsequent reward increases by 3 (PR3). Mice were then trained on a PR7 schedule for one day in a 2-hour session.

**Progressive Ratio-7 Reinforcement**—Following training, mice were tested on PR7 test for 15 consecutive days. PR7 test sessions were 2 hours, however, mice were only allowed to lever press for food for the first 40 min of each session. At the start of PR7 testing, food rewards were switched to 20 mg grain pellets with 1% saccharin and grape flavouring (TestDiet) to allow comparison of reinforcing effects of food consumption outside of the testing session (see below). All mice received exposure to and consumed these grape flavoured pellets in their homecages (50 pellets available) the night prior to the start of tests to limit neophobia.

**Food-restricted group:** Mice in the food-restricted group were tested while tethered to a dummy fibre to ensure that this tether does not interfere with lever pressing activity or with food consumption.

**AGRP neuron stimulation groups:** For the AGRP neuron stimulation groups, mice were returned to *ad lib* food intake for 2 days after training, before initiating testing. Mice were maintained under well-fed conditions. During PR7 test sessions, one group of mice received photostimulation for the whole length of the session (2-h). Within this group, some mice were provided regular chow in their home cages, while others were maintained on the same food used as rewards during the test session for the duration of the experiment. These two subgroups were ultimately combined for statistical analysis because no difference in lever pressing was observed between them. A second group received photostimulation only during the first 40 minutes of the session, when the mice were allowed to press for food. Mice in both photostimulation groups were also tested for lever pressing in the absence of photostimulation after the 15 day test sessions.

**Food restricted with AGRP neuron stimulation group:** After training, a group of food-restricted mice was tested with AGRP neuron photostimulation during a PR7 food reinforcement schedule with photostimulation for the whole length of the session (2 hours). Mice were then returned to *ad lib* food for 2 days, and retested on a PR7 schedule under well-fed conditions without photostimulation.

**No stimulation group:** After training, mice in the no stimulation group were returned to *ad lib* food intake for 2 days, before initiating testing. All mice were maintained under well-fed conditions without photostimulation for testing on a PR7 schedule for 16 consecutive days. Mice were tethered to a dummy fibre during testing.

Mice that did not earn at least 5 food rewards on the first day of PR7 test were removed from the experiment (one mouse from the food-restricted group). Breakpoint was defined as the last ratio completed before 5 min passed without earning a reward. For rate of lever pressing analysis, lever presses were divided into two blocks: first 10 minutes (low-effort work requirement) and rest of session (high-effort work requirement). The first 10 minutes were chosen as low-effort work requirement conditions since average breakpoint time was greater than 10 minutes for all groups.

### Photostimulation-Induced Weight Gain

We noted an increase in body weight during the multi-session AGRP neuron stimulation protocol (Extended Data Fig. 5a), likely due to a long-acting effect of released AGRP<sup>44</sup> following photostimulation (this is not responsible for acute food consumption under investigation here, which is due to the release of Neuropeptide Y and GABA<sup>4,5,45</sup>). To examine whether suppression of lever pressing for food was due to these long-term metabolic changes, we performed control experiments with photostimulation-induced body weight gain separately from interference with negative reinforcement.

AGRP<sup>Chr2</sup> mice were trained to lever press under food restriction as described above. After training, mice were returned to *ad libitum* food for 2 days before testing began. Food rewards were switched to 20 mg grain pellets with 1% saccharine and grape flavouring (TestDiet) during PR7 testing, mirroring the protocol used in the PR7 reinforcement assay above, and only the differences are described. Mice were then tested under PR7 food reinforcement during photostimulation of AGRP neurons. Next, mice underwent the weight gain induction period. Weight gain was induced in one group of mice through daily, 2 hour photostimulation sessions (22 days) until weight gain matched that of the 2-hour photostimulation group in the PR7 test (~28%). A second group did not receive photostimulation, but were tethered to an optic fibre and served as controls for natural weight gain and any potential decline in lever pressing due to the time elapsed between tests. During these sessions, mice did not lever press for food. Mice in both groups were allowed to consume 20 mg grain pellets with 1% saccharine and grape flavouring with the number of rewards each day matched to the average number of rewards on the corresponding session from the 2-hour photostimulation group in the PR7 test. After ~28% weight gain in the photostimulated group, well fed mice were then tested again on a PR7 task during AGRP neuron stimulation.

### Repeated daily AGRP neuron-evoked free feeding assay

To assess the consequences of repeated daily AGRP neuron photostimulation sessions on *ad libitum* food intake, mice were tested as in the PR7 experiment, but pellets were freely delivered without levers present.

### GRIN lens implantation and baseplate fixation

Mice expressing GCaMP6f or GCaMP6s in AGRP neurons were anaesthetized using isoflurane, and a rectangle craniotomy (2-3 mm) was made around viral injection coordinates (bregma, -1.46 mm; midline: 0.3 mm). A customized sharp optical fibre (diameter: 0.6 mm) was inserted to the brain to ~250  $\mu\text{m}$  above the ARC. After retraction of the fibre, a gradient index (GRIN) lens (Part ID: GLP-0584; diameter: 0.5 mm, length: 8.2 mm; Inscopix) with a custom GRIN lens-holder was slowly (150  $\mu\text{m}/\text{min}$ ) implanted. The target depth was determined by observing fluorescent signal through a miniature microscope (nVista HD and HD v2, Inscopix). The GRIN lens was fixed with black dental cement (Lang Dental Manufacturing); then a head bar was fixed with dental cement. A layer of parafilm was covered the top end of the lens. A silicone adhesive (Kwik-Sil; World Precision Instruments) was applied above the parafilm to protect the lens.

Two to four weeks after GRIN lens implantation, awake mice were head-fixed by a head bar holder. A baseplate (Part ID: BPL-1 and Part ID: BPL-2; Inscopix) attached to the miniature microscope was positioned above the GRIN lens. The focal plane was adjusted until neuronal structures and GCaMP6 dynamic responses were clearly observed. Then mice were anaesthetized by isoflurane and the baseplate was fixed with dental cement.

### Calcium imaging in freely moving mice

Mice were habituated to head-fixation and the microscope was connected to the baseplate when the animal was head-fixed followed by 30-min acclimatization before imaging sessions. Fluorescence images were acquired at 10 Hz and the LED power was set 10-35% (0.1-0.35 mW) with analog gain 3-4. To compare the  $\text{Ca}^{2+}$  activity in different test sessions, the image acquisition parameters were set to the same values. Animal behaviour was recorded by a top mounted camera (Basler) (30 Hz). A synchronization signal between the miniature microscope and camera was recorded by a signal acquisition system (Neuralynx).

Ghrelin (1  $\mu\text{g}/\text{g}$ ) and saline injections (i.p.) were performed on AL-fed mice. FR mice (80-85% initial body weight) underwent chow food, false food, and Pavlovian trace conditioning tests. Chow food identical to that in the home cage (see **Mice**). False food was a similar sized wood block/foam plug. For feeding experiments, either object was placed into the test arena 1.5 min after the onset of imaging sessions. For short exposure tests, the object was removed 1 min after delivery. Events of delivery, contact, leaving, and removal were manually marked from the behaviour video. During Pavlovian trace conditioning test, a 200 ms auditory (12 kHz) and visual (blue light) compound CS was randomly presented 60-90 s after the onset of imaging sessions. A lickometer spout was extended 800 ms after the cue with 30 s to access the spout which delivered a palatable liquid food (Ensure). Lick events were recorded by the Neuralynx system.

## Calcium image analysis

All image analyses were performed in ImageJ and Matlab. Because AGRP neurons are at the base of the brain and next to 3<sup>rd</sup> ventricle, the mechanical drift between GRIN lens and brain tissue included some nonlinear distortions. Movement was corrected in Janelia Computer Cluster by a custom Matlab script using an open source toolkit ANTs<sup>46</sup> (<http://picsl.upenn.edu/software/ants/>). The movement-corrected images were cropped to remove the margin values filled by the registration. This movement correction algorithm allowed image analysis even when mice were chewing chow food pellets, typically a difficult case for brain imaging (e.g., Fig. 4f does not show movement artifacts associated with initiation or cessation of chewing). As an example that calcium activity reduction observed during eating is not due to movement artifacts, Fig. 4f shows a neuron (neuron 1) that increases activity and is surrounded by other neurons (3,10,11,12, see Fig. 4d) that reduce activity, indicating that the response properties are due to specific neuron dynamics and not a generalized movement artifact, which would affect the entire local area of the neurons.

To extract calcium indicator fluorescence responses associated with individual neurons, a cell-sorting algorithm<sup>47</sup> based on principal component analysis and independent component analysis was used to automatically compute ROI spatial filters that were applied to the aligned imaging data. Separate spatial filters for each cell consisted of a weight-matrix with values between zero and one that was used to compute the fractional contribution of each pixel to the calculation of calcium fluorescence. Background fluorescence was subtracted from cropped images using ImageJ background subtraction function. Ca<sup>2+</sup> activity of individual cells within ROI spatial filters were extracted from the background subtracted images.  $F/F_0$  was calculated as  $(F-F_0)/F_0$ , where  $F_0$  is the lowest 5% of the fluorescence signal in image sessions on one day. Normalised  $F/F_0$  was used to transform the range of  $F/F_0$  to [0 1] by the equation:  $(F/F_0 - \min(F/F_0)) / (\max(F/F_0) - \min(F/F_0))$ .

ROI spatial filters identified from the same field of view were often different under different test sessions. To compare Ca<sup>2+</sup> activity in such situations, only the intersection of the ROI spatial filters were used to do further analyses and comparisons. Under AL-fed conditions, Ca<sup>2+</sup> activity is quite low, and only few ROIs can be detected by the cell-sorting algorithm. To compare AGRP Ca<sup>2+</sup> activity between AL-fed and other conditions, the ROIs detected under other test conditions with higher GCaMP6 fluorescence were manually mapped to images from the AL-fed condition.

To test whether Ca<sup>2+</sup> activity of individual neurons was changed after ghrelin injection or chow food delivery, 30% of initial mean baseline fluorescence was chosen as a threshold. Neurons with mean fluorescence changes after the experimental manipulation that were more than the threshold, either decreasing or increasing fluorescence, were categorised as changed. For ghrelin administration, the mean fluorescence (from 1-min recording) after ghrelin injection (10-min post-injection) was compared to 1-min mean pre-injection GCaMP6 fluorescence. For food delivery, the mean fluorescence (from 1-min recording) from immediately after food delivery was compared to 1-min mean pre-food GCaMP6 fluorescence.



### Evoked water consumption with SFO neuron activation

For cell type-specific evoked water consumption, *Nos1* was identified as a marker for SFO neurons by inspection of the Allen Brain Atlas. SFO<sup>hM3Dq</sup> and SFO<sup>NOS1-ChR2</sup> mice were housed with *ad libitum* food and water and were transferred into a behavioural arena (Coulbourn Instruments) with food pellets (20 mg each) delivered through an automatic pellet dispenser as previously described. Water was supplied through a ball bearing-gated metal spout that was fed by a water bottle. Licking was detected by beam breaks and calibration experiments showed lick volume was  $1.35 \pm 0.21$  ml ( $n = 2$  mice, mean  $\pm$  s.d.).

All evoked drinking tests were performed during the early light period. Water intake was recorded for one hour prior to the onset of neuron activation to establish a baseline drinking rate. This was followed by a chemogenetic or optogenetic SFO neuron stimulation period. For SFO<sup>hM3Dq</sup> mice, baseline water consumption was measured for one hour followed by Clozapine-*N*-Oxide (Enzo Life Sciences) injection (i.p., 2.5-5 mg/kg). Unless otherwise noted, mice had free access to food and consumption was also measured.

### Progressive ratio-3 reinforcement schedule for water

SFO<sup>hM3Dq</sup> mice that exhibited elevated water consumption in response to CNO (2.5-5 mg/kg, i.p.) were used for instrumental lever-press training (mice that did not show elevated water consumption were determined, *post hoc*, to lack hM3Dq-mCherry expression in the SFO). Training and tests were conducted in operant conditioning chambers (Coulbourn) with two levers, one active and one inactive, at either side of the water dispenser. A pinch valve faucet controlled opening of a syringe tube from which the water was dispensed. For each trial, after reaching lever-press criteria on the active lever, a water reward (4-6  $\mu$ L) was delivered by releasing the pinch valve (NResearch) and was controlled by Graphic State Software (Coulbourn instruments). Lever pressing on the inactive lever was monitored but did not lead to water delivery.

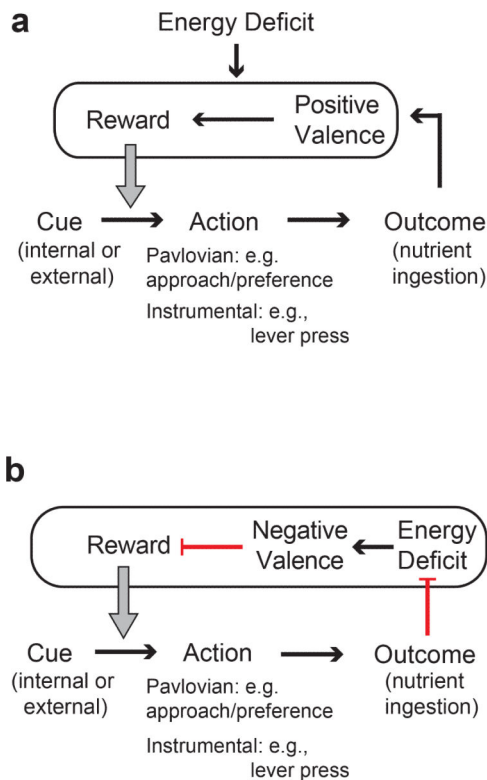
For training, SFO<sup>hM3D</sup> mice were water restricted (1 mL/day) and trained in 30-min daily FR1 sessions until they performed at least 250 lever presses in a session for 3 consecutive days. They were then trained on a progressive ratio-3 (PR3) reinforcement schedule (each water delivery reinforcer required 3 additional lever presses than the previous reinforcer) in 1-hour sessions for three days. Following training, mice were rehydrated by *ad libitum* water access for 1 week. Mice were then tested on a PR3 reinforcement schedule in a 1-h session following CNO (2.5-5 mg/kg) or saline injection. Breakpoint was defined as the last ratio completed before 5 min has passed without earning a water reinforcer.

### Statistics

Values are means  $\pm$  s.e.m. Pairwise comparisons were calculated by unpaired or paired two-tail Students t-test or ANOVA. When equal variance assumptions were violated, nonparametric ANOVA on ranks test was used (see Extended Data Table 1). *Post-hoc* multiple comparisons used Holm-Sidak correction. Statistical analyses and linear regressions were performed using SigmaPlot (Systat) or Matlab. Sample sizes were chosen to cover high and low viral transduction levels. Viral transduction efficiency for mice in electrical activity perturbation experiments (Figs. 1 and 2) was determined *post hoc*, which

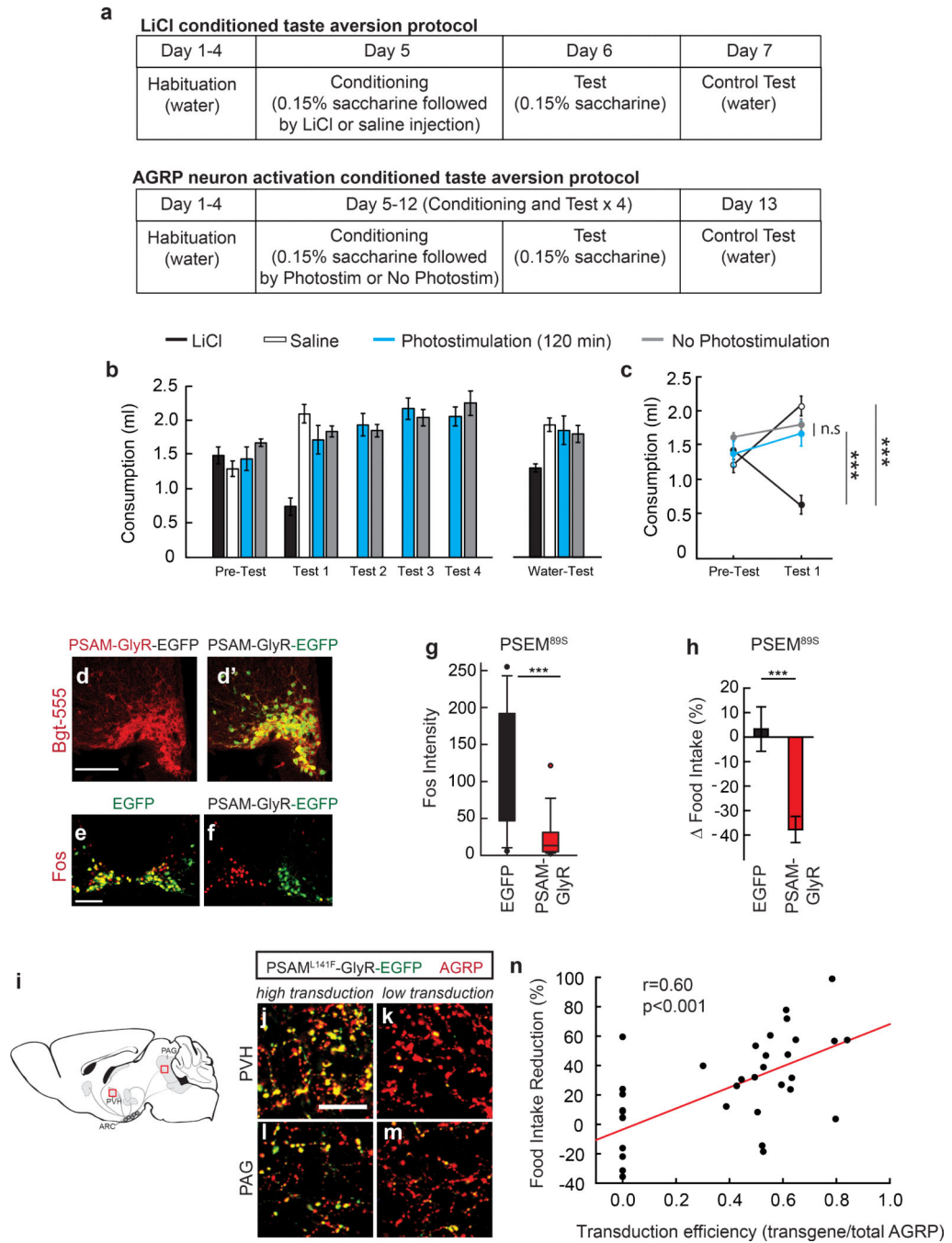
effectively blinded experimenters to the group identity (high or low transduction efficiency) for each subject. Results of statistical tests are summarised in Extended Data Table 1. n.s  $p > 0.05$ , \* $p < 0.05$ , \*\* $p < 0.01$ , \*\*\* $p < 0.001$ .

## Extended Data



### Extended Data Figure 1. Models for homeostatic regulation of learning food preferences and food-seeking behaviors

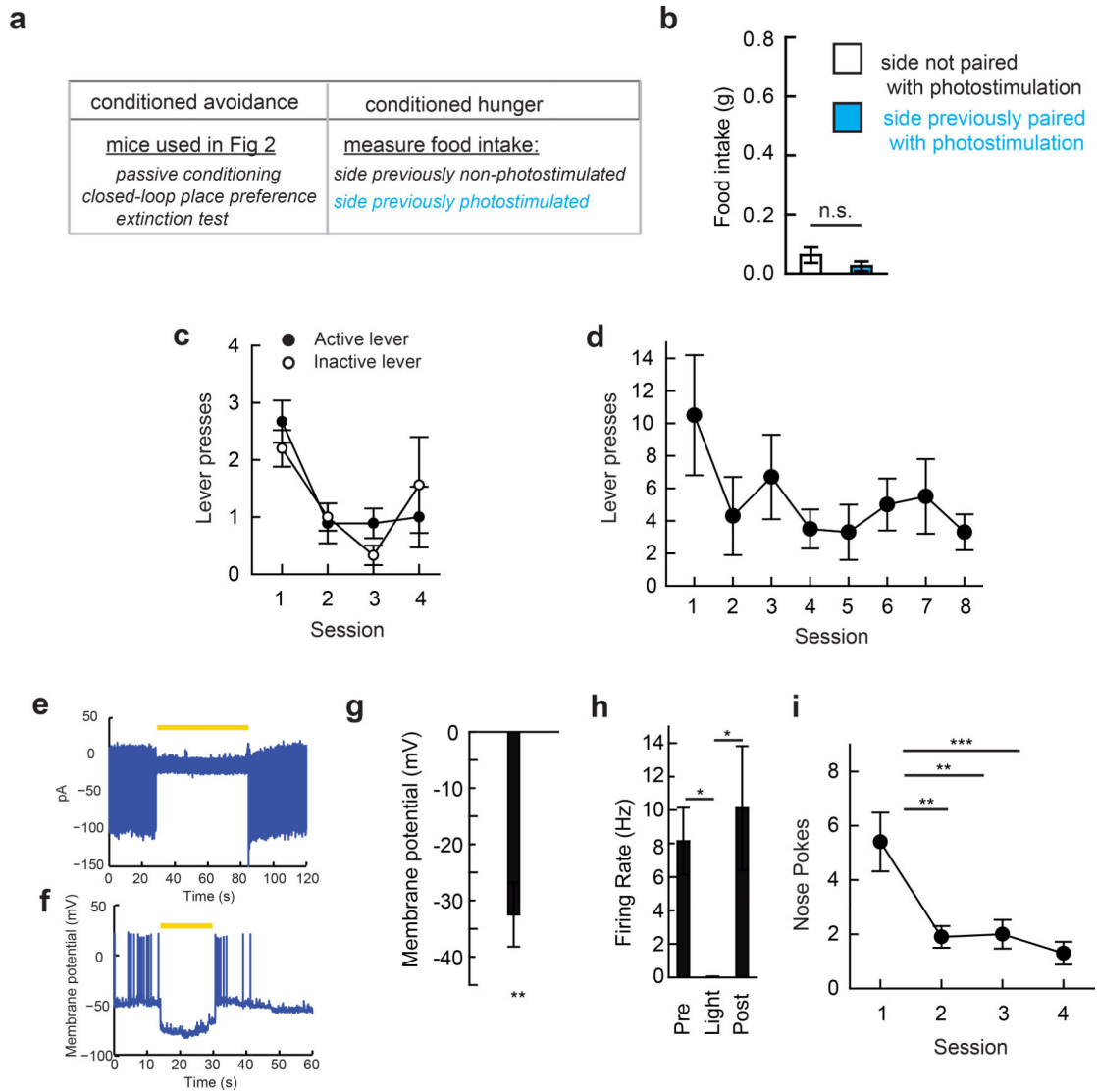
**a**, The relationship between internal or external cues and Pavlovian approach or instrumental food-seeking actions is strengthened by nutrient ingestion. Nutrients have intrinsically positive valence<sup>7</sup> (rewarding), and energy deficit enhances the reward value of outcomes associated with food intake. **b**, Model of food preference and food-seeking in which learning involves reducing an energy deficit internal state that has negative valence. The relationship between internal or external cues and food preferences or food-seeking actions is strengthened by nutrient ingestion outcomes that reduce energy deficit and associated negative valence (red bar arrows are inhibitory). Conversely, the relationship between internal or external cues and food preference or food-seeking actions is weakened if outcomes do not reduce energy deficit.



**Extended Data Figure 2. AGRP neuron activation does not condition taste aversion, and feeding reduction correlates with proportion of AGRP neurons inhibited**

**a**, Experimental design for conditioned taste aversion experiments. Mice were water restricted and habituated to drink water from a spout during 20 min sessions. Four groups of mice were then allowed to consume a tastant (0.15% saccharine solution) for 20 min (Pre-Test) and immediately following this session, they were exposed to a conditioning agent (LiCl, saline, 120-min AGRP neuron photostimulation, or AGRP<sup>ChR2</sup> mice attached to an optical fibre but not photostimulated; all n=6 mice). The next day, mice were tested for consumption of the saccharine solution (Test 1). For AGRP neuron photostimulated and

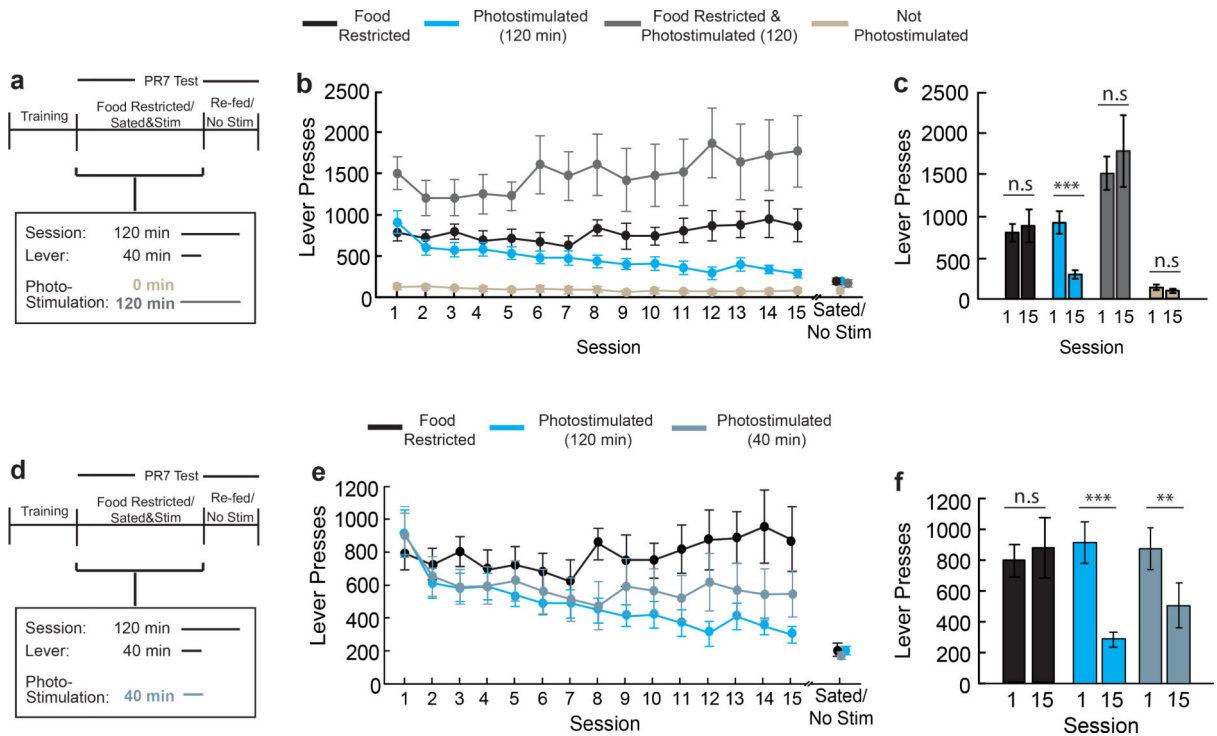
non-photostimulated groups, conditioning and testing was extended with an additional three conditioning and test sessions. The day following the last testing session for each group, water consumption was also measured (Water-Test). **b,c**, Consumption of tastant solution for all sessions (**b**) and comparison for Pre-Test and Test 1 session (**c**). **d,d'**, Confocal micrographs of Cre recombinase-expressing AGRP neurons transduced with rAAV-Syn-FLEX-PSAM<sup>L141F</sup>-GlyR-IRES-EGFP. Alexa555-conjugated-Bungarotoxin (Bgt-555) labels PSAM<sup>L141F</sup>-GlyR (**d**), which co-localizes with EGFP (**d'**). Scale, 100  $\mu$ m. **e,f**, Fos immunofluorescence in the ARC of mice treated with PSEM<sup>89S</sup> during the first 4 hours of the dark period without access to food. AGRP<sup>EGFP</sup> mice (**e**) show high levels of Fos in AGRP neurons and AGRP<sup>PSAM-GlyR</sup> mice (**f**) express low levels of Fos in neurons that express PSAM-GlyR (right side); non-transduced neurons (contralateral side) express high levels of Fos. Scale, 100  $\mu$ m. **g**, Fos immunofluorescence intensity in AGRP neurons from AGRP<sup>PSAM-GlyR</sup> or AGRP<sup>EGFP</sup> mice after PSEM<sup>89S</sup> treatment during the first 4 hours of the dark period without access to food (n=3 mice/condition, n>50 nuclei/condition). **h**, Change in food intake for AGRP<sup>EGFP</sup> mice (n = 12) or AGRP<sup>PSAM-GlyR</sup> mice (n = 23) treated with PSEM<sup>89S</sup> during the first 4 hours of the dark period relative to saline injected on successive days. **i**, Diagram of AGRP neuron axon projection fields showing from where transduction efficiency was calculated. **i-m**, After rAAV-*hSyn-FLEX-rev-PSAM<sup>L141F</sup>-GlyR-IRES-EGFP* transduction of *Agrp-IRES-Cre* mice, measurement of EGFP transduction efficiency in AGRP boutons in the PVH (**i,k**) and PAG (**l,m**). High transduction efficiency (>50% in AGRP boutons) is shown (**i,l**) in comparison to low transduction efficiency (<50% in AGRP boutons) (**k,m**). Scale, 20  $\mu$ m. **n**, Food intake reduction for mice treated with PSEM<sup>89S</sup> is correlated with the transduction efficiency of rAAV-*hSyn-FLEX-rev-PSAM<sup>L141F</sup>-GlyR-IRES-EGFP* in AGRP neurons (EGFP transduced boutons/total AGRP boutons) (n=35 mice). n.s. p>0.05, \*\*\*p<0.001. Values are means  $\pm$  s.e.m.



### Extended Data Figure 3. AGRP neuron activation does not condition appetite or reinforce instrumental responding

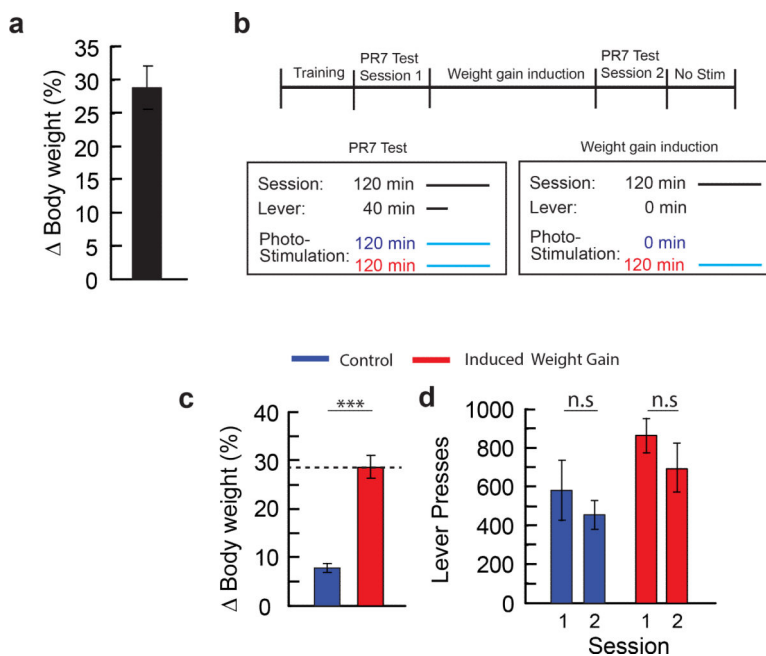
**a**, Experimental design to test conditioned appetite. After closed-loop place preference and extinction testing (Fig. 2), AGRP<sup>ChR2</sup> mice showed reduced occupancy in the photostimulation-paired side of the chamber. Avoidance in extinction indicated conditioning to offset of a negative-valence signal from AGRP neurons. An alternative hypothesis is that induction of food-seeking on the photostimulation side in the absence of food led the mouse to seek food. Because photostimulation was stopped when the mouse passed to the other side of the chamber, this might increase occupancy on the non-photostimulated side. However, this is not consistent with the increased avoidance of the previously photostimulated side in extinction (Fig. 2k) unless the contextual cues previously associated with photostimulation conditioned increased appetite. To test whether conditioned avoidance might be associated with conditioned hunger, we measured food intake in AL-fed mice after closed-loop place preference, and extinction tests in Fig. 2g-k on each side of the apparatus in the absence of photostimulation. **b**, Mice did not show conditioned food

consumption on the previously photostimulated side (paired t-test,  $n=8$  mice). This indicates that avoidance observed in extinction was not a consequence of food-seeking behaviors being differentially engaged on one side of the apparatus. **c,d** Cessation of AGRP neuron photostimulation did not condition instrumental responding. **(c)** Nose pokes by AL-fed  $AGRP^{ChR2}$  mice ( $n=9$ ) during photostimulation, where a nose poke gives a 20 s pause in light pulses for each behavioral session. Nose pokes reduced across sessions indicating the absence of instrumental conditioning. Filled circles: active port, empty circles: inactive port. **(d)** For AL-fed  $AGRP^{ChR2}$  mice previously trained to hit a lever for food, lever presses during photostimulation, where a lever press gives a 20 s pause in light pulses for each behavioral session (repeated measures ANOVA  $F(7,40)=1.19$ ,  $p=0.330$ ;  $n=8$  mice). **e-h**, For optogenetic silencing with Arch (550-600 nm, 8-11 mW/mm<sup>2</sup>), **(e)** cell-attached recording of AGRP neuron firing rate in brain slices from *Agrp-IRES-Cre;Ai35d* ( $AGRP^{Arch}$ ) mice during light illumination. **(f)** Whole cell recording of  $AGRP^{Arch}$  during optogenetic inhibition. **(g)** Membrane potential change in AGRP neurons expressing Arch during light illumination ( $n=6$ ). **(h)** AGRP neuron firing rate during optogenetic inhibition of Arch-expressing AGRP neurons ( $n=4$ ). **i**, Optogenetic silencing of AGRP neurons in food-restricted mice did not condition free operant instrumental responding. Nose pokes by  $AGRP^{Arch}$  mice resulted in 60-s of 561 nm light delivered to an optical fibre over the ARC. Nose poking reduced over multiple sessions (ANOVA  $F(3,24)=7.835$ ,  $p<0.001$ ;  $n=7$  mice), indicating that silencing AGRP neurons did not directly reinforce instrumental responding. n.s.  $p>0.05$  Values are means  $\pm$  s.e.m.



**Extended Data Figure 4. Lever pressing for food is sensitive to AGRP neuron photostimulation duration**

**a**, Experimental design of progressive ratio 7 lever-press experiment from Fig. 3 for a FR AGRP neuron photostimulated group and an AL-fed non-photostimulated group. The two additional groups of mice were trained to lever press in food-restriction on a PR7 reinforcement schedule. For the food-restricted with photostimulation group, mice were maintained on food-restricted and tested with PR7 reinforcement tests over 15 sessions with photostimulation. Each session was 2-h, where levers were available for the first 40 minutes of the session, and photostimulation was delivered for the length of the session (120 min, grey). Mice were then *ad libitum* re-fed and tested on a non-photostimulated PR7 session. For the AL-fed non-photostimulated group, mice were *ad libitum* re-fed following lever-press training and tested with PR7 reinforcement tests over 16 sessions, with no photostimulation delivered (beige). **b**, Lever presses for each PR7 session for FR AGRP neuron photostimulated mice (grey, n=11) mice and AL-fed non-photostimulated mice (beige, n=8). For comparison, data are shown for food-restricted and 120-min-photostimulated groups that are reproduced from Fig. 3b. **c**, Lever presses on first (1) and last (15) sessions in PR7 test for food-restricted with photostimulation mice (grey) mice and sated no photostimulation mice (beige). Also shown are data for food-restricted and 120-min-photostimulated groups that are reproduced from Fig. 3c. **e**, Experimental design of progressive ratio 7 lever-press experiment from Fig. 3 for a 40-min photostimulation group. One additional group of mice was trained to lever press in food-restriction on a PR7 reinforcement schedule. Mice were then *ad libitum* re-fed and tested with PR7 reinforcement tests over 15 sessions. Each session was 2-h, where levers were available for the first 40 minutes of the session, and photostimulation was delivered only while levers were available (grey). A non-photostimulated PR7 session was also performed after the 15<sup>th</sup> test session. **f**, Lever presses for each PR7 session for 40-min-photostimulated (grey, n=12) mice. Also shown are data for food-restricted and 120-min-photostimulated groups that are reproduced from Fig. 3b. **g**, Lever presses on first (1) and last (15) sessions in PR7 test for 40-min-photostimulated mice (grey). Also shown are data for food-restricted and 120-min-photostimulated groups that are reproduced from Fig. 3c. n.s.  $p > 0.05$ , \*\* $p < 0.01$ , \*\*\* $p < 0.001$ . Values are means  $\pm$  s.e.m.

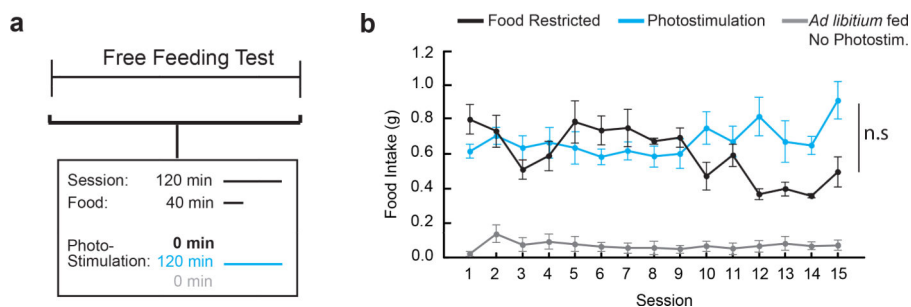


#### Extended Data Figure 5. AGRP neuron-associated body weight increase does not suppress AGRP neuron-evoked food-seeking

**a**, Weight gain for the 120-min AGRP neuron photostimulated ( $n=11$ ) group in the PR7 experiment (from Fig. 3) after 15 sessions. Weight gain is due to eating after the test session when the mouse is returned to the homecage and is associated with long-lasting effects from release of AGRP<sup>44</sup>. Previous experiments have shown that AGRP is not responsible for the acute feeding behavior investigated in this study<sup>4,5,45</sup>. However, metabolic changes associated with weight gain could be an alternative cause of reduced instrumental food-seeking shown in Fig. 3. To test the effect of weight gain in mice trained to lever press for food on a PR7 reinforcement schedule, we induced weight gain without the negative reinforcement extinction protocol from Fig. 3. **b**, Experimental design of progressive ratio-7 lever-press experiment with AGRP neuron photostimulation-induced weight gain but lacking disruption of negative reinforcement during food-seeking. AGRP<sup>ChR2</sup> mice were trained under food deprivation to lever press under a PR7 schedule for food pellets. After training, both groups were *ad libitum* re-fed, and the mice were divided into two groups: 1) control mice with no induction of weight gain (blue) and 2) the induced weight gain group (red). Both groups were then tested on a PR7 reinforcement schedule under AGRP neuron photostimulation conditions (PR7 Test 1). Following this session, a photostimulation-induced weight gain protocol was initiated for the second group. Mice received one 2-h experimental session per day, where they were photostimulated for the whole experimental session and body weight was monitored daily. During these sessions, levers were not available, but free food was provided during these sessions (the amount of food was matched in quantity to the average amount of food acquired by the 120 min photostimulation group under the PR7 experiment from Fig. 3 for the corresponding session). The photostimulation-induced weight gain protocol was conducted for 22 consecutive days, which was required for percent body weight gain to be comparable to levels acquired by the 120-min AGRP neuron photostimulation group in the PR7 experiment

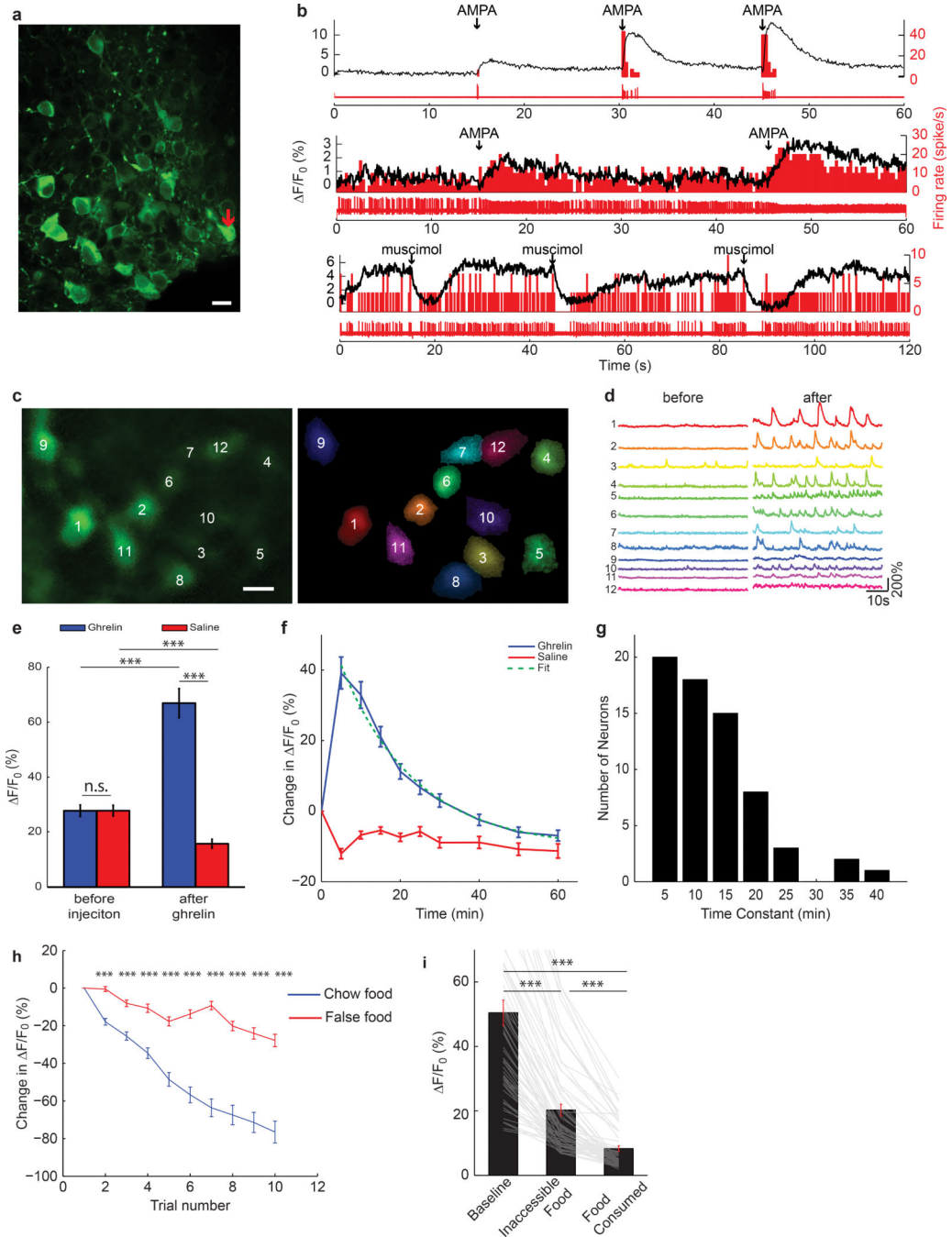


(~28%) from Fig 3. Control mice were tethered to a fibre but did not receive photostimulation, otherwise they received the same experimental manipulation as induced weight gain mice (access to the same amount of food), and their body weight was also monitored. After the induced weight gain group achieved a 28% weight gain, a second PR7 test was conducted for both groups in the same manner as the first one. **c**, Percent body weight change for control (blue, n=6) and induced weight gain (red, n=6) mice. Grey dotted line: percent body weight change for photostimulated mice in PR7 experiment from Fig. 3. **d**, Lever presses for control (blue) and AGRP neuron photostimulation-induced weight gain (red) mice on first (1) and second (2) PR7 test, prior and after weight gain induction protocol, respectively. There is no significant reduction in lever pressing between PR7 sessions within either group. n.s.  $p > 0.05$ , \*\*\* $p < 0.001$ . Values are means  $\pm$  s.e.m.



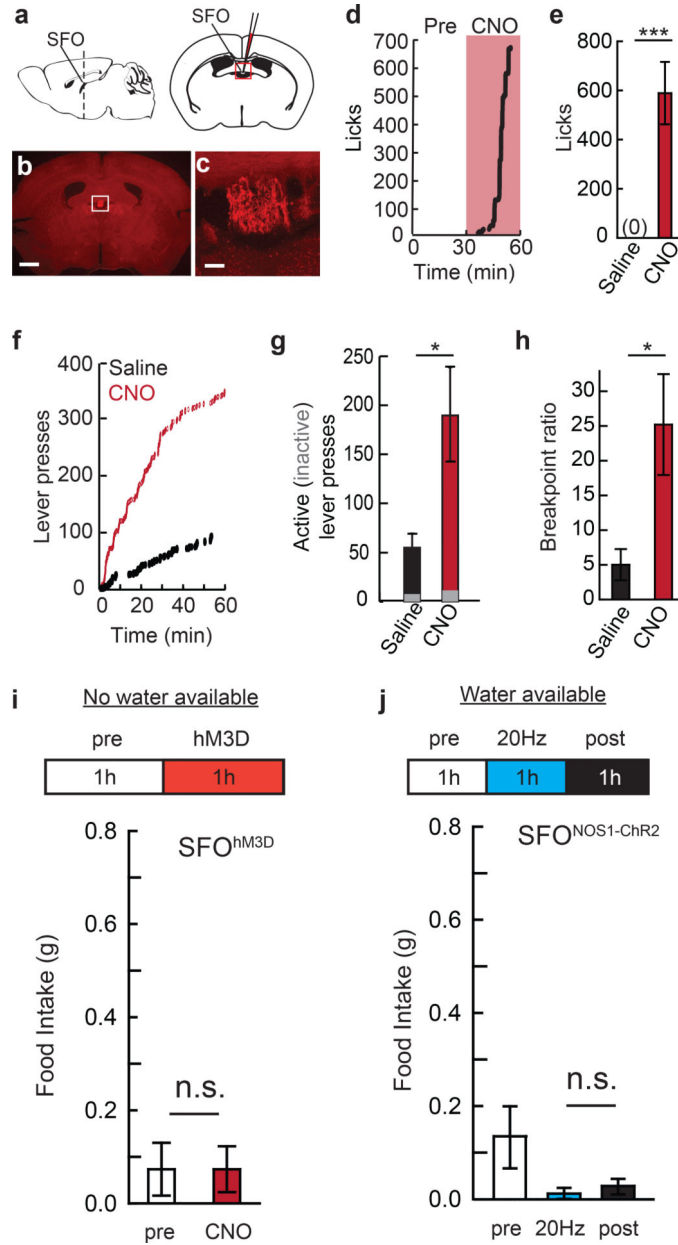
**Extended Data Figure 6. Free food consumption is not reduced with repeated daily AGRP neuron photostimulation sessions**

**a**, Experimental design of free feeding experiment over repeated sessions. Three groups of AGRP<sup>Chr2</sup> mice were tested on a 15 session free feeding protocol (no lever pressing required) either under food restriction (black), *ad libitum* fed AGRP neuron photostimulated (cyan), or *ad libitum* fed without AGRP neuron photostimulation (grey) conditions. On each day, mice received one 2-hour session, where food was freely available for the first 40 minutes of the session. AGRP neuron photostimulated group received photostimulation for the entire 2 hour session (cyan). **b**, Food intake for each session of the free feeding experiment for food restricted (black, n=6), AGRP neuron 120-min-photostimulated (cyan, n=6), and no photostimulation (grey, n=6) groups. n.s.  $p > 0.05$ . Values are means  $\pm$  s.e.m.



**Extended Data Figure 7. Calcium imaging of AGRP neurons in freely moving mice**  
**a**, Projection of confocal images of AGRP neurons from brain slices after mice expressed GCaMP6s for 10 months after viral injection. >99.5% neurons show nuclear exclusion of GCaMP6s, indicating good cell health. Red arrow, rare example of filled nucleus. Scale bar, 15  $\mu$ m. **b**, In AGRP neurons, characterization of the relationship between action potential firing rate (cell attached recordings) and change of GCaMP6f fluorescence activity in brain slices by puffing AMPA for activation (top, middle) or muscimol for inhibition (bottom). **c**, Epifluorescence images of AGRP<sup>GCaMP6f</sup> neurons (left) from AL-mice after ghrelin

injection by deep-brain calcium imaging and their ROI spatial filters (right) for image analysis. Scale bar, 15  $\mu\text{m}$ . **d**, For freely moving AL-fed mice during *in vivo* imaging, fluorescence traces of individual  $\text{AGRP}^{\text{GCaMP6f}}$  neurons in **(c)** before and after ghrelin injection (fluorescence responses separated in time by 4 min, during which time ghrelin was injected). **e**, Changes in mean  $\text{Ca}^{2+}$  activity before and 4 min after ghrelin/saline injections (90 neurons, 4 AL-fed mice). **f**, Time course of changes in mean  $\text{Ca}^{2+}$  activity after ghrelin (blue) or saline (red) injection (90 neurons, 4 mice). Green dashed line: exponential fit. **g**, Distribution of individual time constants for decline of ghrelin-mediated fluorescence increase for individual neurons showing goodness of fit  $>0.85$  (67/90 neurons, 4 mice). **h**, Baseline GCaMP6f fluorescence at the start of each trial before 1 min exposure to food/wood in each trial. **i**, GCaMP6f fluorescence comparing initial baseline activity, exposure to an inaccessible but visible food outside the cage, and subsequent consumption of food (60 neurons, 2 mice). n.s.  $p>0.05$ , \*\*\* $p<0.001$ . Multiple comparisons with Holm's correction. Values are means  $\pm$  s.e.m.



**Extended Data Figure 8. SFO neuron-evoked water seeking and consumption**

**a**, Schematic of injection targeting of hM3Dq-mCherry to SFO neurons. **b**, Epifluorescence image of mCherry fluorescence in a coronal section containing the SFO (box) targeted stereotaxically by co-injection of rAAV-*hSyn*-Cre and rAAV-*Efla*-DIO-hM3Dq-mCherry. Scale bar, 1 mm. **c**, Confocal micrograph of SFO neurons co-transduced with rAAV-*hSyn*-Cre and rAAV-*Efla*-DIO-hM3Dq-mCherry. Scale, 100  $\mu$ m. **d**, Number of licks for a representative SFO<sup>hM3Dq</sup> mouse during evoked water consumption following activation of SFO neurons by CNO injection. **e**, Number of licks for SFO<sup>hM3Dq</sup> mice following saline or CNO injection (n=5 mice). **f**, Cumulative lever pressing for a SFO<sup>hM3Dq</sup> mouse following injection of CNO (red) or saline (black). **g,h**, For SFO<sup>hM3Dq</sup> mice, lever presses (red/black: active lever, grey: inactive lever) (**g**) and breakpoint reinforcement ratio (**h**) on a PR-3 water

reinforcement schedule following either saline or CNO injection (n = 5 mice). **i**, (top) Experimental design to test if activation of SFO neurons can elicit food consumption in the absence of water. SFO<sup>hM3D</sup> mice were presented with access to food but not water for one hour (pre), which was followed by CNO injection, and food intake was measured for an additional hour. (bottom) Food intake by SFO<sup>hM3D</sup> mice that lack access to water before (pre) and after the application of CNO (paired t-test, n=3). **k**, (top) Experimental design to test if activation or offset of SFO neurons elevate food consumption behavior. SFO<sup>NOS1-ChR2</sup> mice had access to food and water, and both were measured before (1-h, pre), during (20 Hz, 1-h), and after photostimulation (1-h, post). (bottom) Food consumed by SFO<sup>NOS1-ChR2</sup> mice before (pre), during (20 Hz), or after (post) photostimulation (paired t-test, n=5). n.s. p>0.05. Values are means ± s.e.m.

Extended Data Table 1

Results of statistical analyses.

Figure	Sample size (n)	Statistical Test	Values
1f	EGFP: 6; ChR2:8	Unpaired t-test	p=0.03
1j	low: 13; high: 16	Unpaired t-test	p<0.001
1k	low: 13; high: 16	Unpaired t-test	p=0.005
1l	29	Pearson Correlation	r=0.74, p<0.001
1m	<30%: 15 >30%: 14	2-WAY RM ANOVA factor 1: (group) <30% v. >30% factor 2: pre/post session Interaction: group × session Post hoc multiple comparisons, with Holm-Sidak corrections	F(1,27)=5.6, p=0.025 F(1,27)=3.9, p=0.06 F(1,27)=28.5, p<0.001 <30%: p=0.041; >30% p<0.001 pre: p=0.36; post: p<0.001
2c	EGFP-FR: 13; PSAM- GlyR-FR: 20 PSAMGlyR-FR: 20; AL: 9	Unpaired t-test Unpaired t-test	p=0.036 p=0.024
2d	26	Pearson Correlation	r=0.58, p=0.002
2e	35	Pearson Correlation	r=0.56; p<0.001
2f	8	Pearson Correlation	r=0.81, p=0.014
2i	12 per group	2-WAY RM ANOVA; Factor 1: (group) AGRP-ChR2 v. AGRP-GFP Factor 2: session Interaction: group × session Post hoc mult. comparisons. Holm-Sidak corrections. Session 7	F(1,154)=3.0, p=0.097 F(7,154)=2.3, p=0.029 F(7,154)=3.3, p=0.003 p=0.003
2j	12 per group	2-WAY RM ANOVA; Factor 1: (group) AGRP-ChR2 v. AGRP-GFP Factor 2: session Interaction: group × session Post hoc mult. comparisons. Holm-Sidak corrections. Session 4 Session 5; Session 6; Session 7	F(1,154)=6.4, p=0.019 F(7,154)=3.2, p=0.004 F(7,154)=3.8, p<0.001 p=0.025 p=0.009; p=0.035; p<0.001
2k	ChR2: 12, EGFP: 12	Unpaired t-test	p=0.025
3b	Food Restriction: 11 Photostimulation: 11	2-WAY RM ANOVA; Factor 1: (Group) Restricted v. Photostim. Factor 2: Session Interaction: group × session Post hoc mult. comparisons. Holm-Sidak corrections. Session 3 Session 8; Session 10 Session 11; Session 12	F(1,280)=7.90, p=0.011 F(14,280)=1.76, p=0.045 F(14,280)=2.97, p<0.001 p=0.047 p=0.015; p=0.048 p=0.002; p<0.001 p=0.014; p=0.003; p<0.001

Figure	Sample size (n)	Statistical Test	Values
		<i>Session 13; Session 14; Session 15</i>	
3c	Food Restriction: 11; Photostimulation: 11	Paired t-test	Food Restricted: p=0.682; Photostim: p<0.001
3d	Food Restriction: 11; Photostimulation: 11	Paired t-test	Food Restricted: p=0.821; Photostim: p<0.001
3e	Food Restriction: 11; Photostimulation: 11	Paired t-test	Food Restricted: p=0.385; Photostim: p=0.002
3g	Food Restriction: 11 Photostimulation: 11	2-WAY RM ANOVA; Food Restricted group; Factor 1: Session <i>Factor 2: Time Block</i> <i>Interaction: Session vs Time Block</i> Photostimulated group; Factor 1: Session <i>Factor 2: Time Block</i> <i>Interaction: Session vs Time Block</i> Post hoc multiple comparisons with Holm-Sidak corrections <i>Session 1: First 10 min vs Rest of Session</i> <i>Session 15: First 10 min vs Rest of Session</i> <i>First 10 min: Session 1 vs Session 15</i> <i>Rest of Session: Session 1 vs Session 15</i>	F(1,10)=1.29, p=0.282 F(1,10)=3.99, p=0.074 F(1,10)=5.20, p=0.046 F(1,10)=34.15, p<0.001 F(1,10)=27.94, p<0.001 F(1,10)=7.55, p=0.021 Food Restricted: p=0.357; Photostim: p=0.076 Food Restricted: p=0.009; Photostim: p<0.001 Food Restricted: p=0.045; Photostim: p=0.006 Food Restricted: p=0.824; Photostim: p<0.001
4e	61 neurons, 4 mice	Paired t-test	p<0.001
4i	110 neurons, 4 mice	RM ANOVA on RANKS Post hoc multiple comparisons (Holm-Sidak) <i>1st trial base v. 1st trial food</i> <i>1st trial base v. satiety</i> <i>1st trial food v. satiety</i>	p<0.001 p<0.001 p<0.001 p<0.001
4l	Before: 60 neurons; After: 65 neurons; 3 mice	<i>Unpaired t-test</i>	p<0.001
5d	8	Paired t-test	5Hz: p=0.002; 10Hz: p<0.001; 20Hz: p<0.001
5e	Control: 6 ChR2: 12	2-WAY RM ANOVA; Factor 1: (group) NOS1-ChR2 v. C57B6/J <i>Factor 2: session</i> <i>Interaction: group × session</i> Post hoc multiple comparisons (Holm-Sidak); Session 2 <i>Session3; Session 4</i> <i>Session 5-7</i>	F(1,112)=26.2, p<0.001 F(7,112)=0.74, p=0.64 F(7,112)=4.25, p<0.001 p=0.003 p<0.001; p=0.001 p<0.001
5g	Control: 6, ChR2: 12	Unpaired t-test	p=0.003
ED 2c	LiCl:6 Saline: 6 Photostimulation: 6 No Photostimulation: 6	2-WAY RM ANOVA; Factor 1: group (LiCl, Sal., Photo, No Photo) <i>Factor 2: session</i> <i>Interaction: group × session</i> Post hoc mult. comparisons (Holm-Sidak); LiCl v. Photostimulation <i>LiCl v. Saline</i> <i>Photostimulation v. No photostimulation</i>	F(3,20)=5.76, p=0.005 F(1,20)=4.47, p=0.047 F(3,20)=29.247, p<0.001 p<0.001 p<0.001 p=0.517
ED 2g	3 mice, >50 nuclei/ condition	Mann-Whitney U-Test	p<0.001
ED 2h	EGFP: 12; PSAM-GlyR: 23	Unpaired t-test	p<0.001
ED 2n	35	Pearson Correlation	r=0.60, p<0.001
ED 3b	8 mice	Paired t-test	p=0.44
ED 3c	9 mice	2-WAY RM ANOVA; Factor 1: (group) Active v. Inactive lever <i>Factor 2: session</i> <i>Interaction: group × session</i>	F(1,24)=0.571, p=0.471 F(3,24)=4.681, p=0.01 F(3,24)=1.69, p=0.196

Figure	Sample size (n)	Statistical Test	Values
ED 3d	8 mice	1-Way RM ANOVA	F(7,40)=1.19, p=0.330
ED 3g	6 cells	t-test	p=0.002
ED 3h	4 cells	Unpaired t-test	pre v. light: p=0.029; light v. post: p=0.029
ED 3i	7 mice	1-Way RM ANOVA	F(3,24)=7.835, p<0.001
ED 4b	Food Restriction: 11 Photostim. (120 min): 11 Food Rest & Photostim: 11; Sated No Photostim: 8	2-WAY RM ANOVA; Factor1: Group (Restr., Photo R&Photo, NoPhoto) Factor 2: Session Interaction group × session	F(3,518)=38.86, p<0.001 F(14,518)=2.719, p<0.001 F(42,518)=1.598, p=0.012
ED 4c	Food Restriction: 11 Photostim. (120 min): 11 Food Rest & Photostim: 11 Sated No Photostim: 8	Paired t-tests	Food Restricted: p=0.682 Photostim. (120 min): p<0.001 Food Rest & Photostim: p=0.44 Sated No Photostim: p=0.225
ED 4e	Food Restriction: 11 Photostim. (120 min): 11 Photostim. (40 min): 12	2-WAY RM ANOVA; Factor1: Group (Restr., Photo-40, Photo-120) Factor 2: Session Interaction group × session	F(2,434)=3.04, p=0.063 F(14,434)=3.52, p<0.001 F(28,434)=2.08, p=0.001
ED 4f	Food Restriction: 11 Photostim. (120 min): 11 Photostim. (40 min): 12	Paired t-tests	Food Restricted: p=0.682 Photostim. (120 min): p<0.001 Photostim. (40 min): p=0.002
ED 5c	6 per group	Unpaired t-test	p<0.001
ED 5d	6 per group	Paired t-test	Control: p=0.40; Induced Weight Gain: p=0.084
ED 6b	6 per group	2-WAY RM ANOVA; Factor 1: (group) Rest. v. Photostim Factor 2: session Interaction: group × session	F(1,140)=1.069, p=0.326 F(14,140)=2.380, p=0.005 F(14,140)=6.628, p<0.001
ED 7e	90 neurons, 4 mice	2-WAY RM ANOVA; Factor 1: time (before,after) Factor 2: group (saline,ghrelin) Interaction: time×group Post hoc mult. comparisons (Holm- Sidak); Before: saline v ghrelin After: saline v ghrelin Saline: before v after Ghrelin: before v after	F(1,88)=43.641, p<0.001 F(1,88)=0.245,p=0.622 F(1,88)=155.805,p<0.001 p=0.894 p<0.001 p<0.001 p<0.001
ED 7h	57 neurons, 2 mice	Multiple comparisons (Holm-Sidak correction); Trials 2-10	p<0.001
ED 7i	60 neurons, 2 mice	RM ANOVA on RANKS Post hoc multiple comparisons (Holm- Sidak); base v. inaccessible base v. food; inaccessible v. food	p<0.001 p<0.001 p<0.001; p<0.001
ED 8e	5	Paired t-test	p<0.001
ED 8g	5	Paired t-test	p=0.027
ED 8h	5	Paired t-test	p=0.028
ED 8i	3 mice	Paired t-test	p=0.95
ED 8j	5 mice	Paired t-test	p=0.48

## Supplementary Material

Refer to Web version on PubMed Central for supplementary material.

## Acknowledgments

This research was funded by the Howard Hughes Medical Institute. Z.F.H.C. was funded by the HHMI Janelia Farm Graduate Scholar program. We thank B. Balleine, M. Schnitzer, N. Ji, A. Lee, Z. Guo for suggestions on experimental design; H. Su for molecular biology; J. Rouchard, S. Lindo, K. Morris, M. McManus for mouse breeding and procedures; M. Copeland for histology; J. Osborne and C. Werner for apparatus design; K. Branson for automated mouse tracking software (Ctrax); J. Dudman, S. Eddy, H. Grill, N. Geary, U. Heberlein for comments on the manuscript.

## References

1. van den Top M, Lee K, Whyment AD, Blanks AM, Spanswick D. Orexigen-sensitive NPY/AgRP pacemaker neurons in the hypothalamic arcuate nucleus. *Nat. Neurosci.* 2004; 7:493–494. [PubMed: 15097991]
2. Krashes MJ, et al. Rapid, reversible activation of AgRP neurons drives feeding behavior in mice. *J Clin Invest.* 2011; 121:1424–1428. [PubMed: 21364278]
3. Luquet S, Perez FA, Hnasko TS, Palmiter RD. NPY/AgRP neurons are essential for feeding in adult mice but can be ablated in neonates. *Science.* 2005; 310:683–685. [PubMed: 16254186]
4. Aponte Y, Atasoy D, Sternson SM. AGRP neurons are sufficient to orchestrate feeding behavior rapidly and without training. *Nat. Neurosci.* 2011; 14:351–355. [PubMed: 21209617]
5. Atasoy D, Betley JN, Su HH, Sternson SM. Deconstruction of a neural circuit for hunger. *Nature.* 2012; 488:172–177. [PubMed: 22801496]
6. Sternson SM. Hypothalamic survival circuits: blueprints for purposive behaviors. *Neuron.* 2013; 77:810–824. [PubMed: 23473313]
7. Yiin YM, Ackroff K, Sclafani A. Flavor preferences conditioned by intragastric nutrient infusions in food restricted and free-feeding rats. *Physiol. Behav.* 2005; 84:217–231. [PubMed: 15708774]
8. Dickinson, A.; Balleine, B. Stevens' Handbook of Experimental Psychology. Gallistel, R., editor. Vol. 3. John Wiley & Sons, Inc.; 2002. p. 497-533.Ch. 12
9. Rescorla RA, Solomon RL. Two-process learning theory: Relationships between Pavlovian conditioning and instrumental learning. *Psychol Rev.* 1967; 74:151–182. [PubMed: 5342881]
10. Mackintosh, NJ. Conditioning and associative learning. Oxford University Press; 1983.
11. Berridge KC. Motivation concepts in behavioral neuroscience. *Physiol. Behav.* 2004; 81:179–209. [PubMed: 15159167]
12. Cabanac M. Physiological role of pleasure. *Science.* 1971; 173:1103–1107. [PubMed: 5098954]
13. Robinson MJ, Berridge KC. Instant transformation of learned repulsion into motivational “wanting”. *Curr. Biol.* 2013; 23:282–289. [PubMed: 23375893]
14. Hull, CL. Principles of Behavior. D. Appleton-Century Co.; 1943.
15. Navratilova E, et al. Pain relief produces negative reinforcement through activation of mesolimbic reward-valuation circuitry. *Proc. Natl. Acad. Sci. U. S. A.* 2012; 109:20709–20713. [PubMed: 23184995]
16. Sidman M. Avoidance conditioning with brief shock and no exteroceptive warning signal. *Science.* 1953; 118:157–158. [PubMed: 13076224]
17. Margules DL, Olds J. Identical “feeding” and “rewarding” systems in the lateral hypothalamus of rats. *Science.* 1962; 135:374–375. [PubMed: 14469788]
18. Jennings JH, Rizzi G, Stamatakis AM, Ung RL, Stuber GD. The inhibitory circuit architecture of the lateral hypothalamus orchestrates feeding. *Science.* 2013; 341:1517–1521. [PubMed: 24072922]
19. Stunkard AJ, Rush J. Dieting and depression reexamined. A critical review of reports of untoward responses during weight reduction for obesity. *Ann. Intern. Med.* 1974; 81:526–533. [PubMed: 4606433]
20. Keys, A.; Brozek, J.; Henshel, A.; Mickelsen, O.; Taylor, HL. The biology of human starvation. Vol. II. University of Minnesota Press; 1950.
21. Wadden TA, Stunkard AJ, Smoller JW. Dieting and depression: a methodological study. *Journal of consulting and clinical psychology.* 1986; 54:869–871. [PubMed: 3794038]



22. Takahashi KA, Cone RD. Fasting induces a large, leptin-dependent increase in the intrinsic action potential frequency of orexigenic arcuate nucleus neuropeptide Y/Agouti-related protein neurons. *Endocrinology*. 2005; 146:1043–1047. [PubMed: 15591135]
23. Betley JN, Cao Zhen Fang H, Ritola Kimberly D, Sternson Scott M. Parallel, Redundant Circuit Organization for Homeostatic Control of Feeding Behavior. *Cell*. 2013; 155:1337–1350. [PubMed: 24315102]
24. Magnus CJ, et al. Chemical and genetic engineering of selective ion channel-ligand interactions. *Science*. 2011; 333:1292–1296. [PubMed: 21885782]
25. Cravens RW, Renner KE. Conditioned hunger. *J. Exp. Psychol.* 1969; 81:312–316. [PubMed: 5811807]
26. Ghosh KK, et al. Miniaturized integration of a fluorescence microscope. *Nat Methods*. 2011; 8:871–878. [PubMed: 21909102]
27. Chen TW, et al. Ultrasensitive fluorescent proteins for imaging neuronal activity. *Nature*. 2013; 499:295–300. [PubMed: 23868258]
28. Johnson RF, Beltz TG, Thunhorst RL, Johnson AK. Investigations on the physiological controls of water and saline intake in C57BL/6 mice. *Am. J. Physiol. Regul. Integr. Comp. Physiol.* 2003; 285:R394–403. [PubMed: 12714354]
29. Oka Y, Ye M, Zuker CS. Thirst driving and suppressing signals encoded by distinct neural populations in the brain. *Nature*. 2015
30. Chen Y, Lin YC, Kuo TW, Knight ZA. Sensory detection of food rapidly modulates arcuate feeding circuits. *Cell*. 2015; 160:829–841. [PubMed: 25703096]
31. Olds, J. Brain stimulation and motivation: research and commentary. Valenstein, ES., editor. Scott, Foresman and Company; 1973. p. 81-99.
32. Jennings JH, et al. Visualizing hypothalamic network dynamics for appetitive and consummatory behaviors. *Cell*. 2015; 160:516–527. [PubMed: 25635459]
33. Saper CB, Chou TC, Elmquist JK. The need to feed: homeostatic and hedonic control of eating. *Neuron*. 2002; 36:199–211. [PubMed: 12383777]
34. Domingos AI, et al. Leptin regulates the reward value of nutrient. *Nat. Neurosci.* 2011; 14:1562–1568. [PubMed: 22081158]
35. Egecioglu E, et al. Ghrelin increases intake of rewarding food in rodents. *Addict. Biol.* 2010; 15:304–311. [PubMed: 20477752]
36. Wang Q, et al. Arcuate AgRP neurons mediate orexigenic and glucoregulatory actions of ghrelin. *Molecular metabolism*. 2014; 3:64–72. [PubMed: 24567905]
37. Yang Y, Atasoy D, Su HH, Sternson SM. Hunger states switch a flip-flop memory circuit via a synaptic AMPK-dependent positive feedback loop. *Cell*. 2011; 146:992–1003. [PubMed: 21925320]
38. Krashes MJ, et al. An excitatory paraventricular nucleus to AgRP neuron circuit that drives hunger. *Nature*. 2014; 507:238–242. [PubMed: 24487620]
39. Rolls BJ, et al. Thirst following water deprivation in humans. *Am. J. Physiol.* 1980; 239:R476–482. [PubMed: 7001928]
40. Atasoy D, Aponte Y, Su HH, Sternson SM. A FLEX switch targets Channelrhodopsin-2 to multiple cell types for imaging and long-range circuit mapping. *J. Neurosci.* 2008; 28:7025–7030. [PubMed: 18614669]
41. Tsai HC, et al. Phasic firing in dopaminergic neurons is sufficient for behavioral conditioning. *Science*. 2009; 324:1080–1084. [PubMed: 19389999]
42. Branson K, Robie AA, Bender J, Perona P, Dickinson MH. High-throughput ethomics in large groups of *Drosophila*. *Nat Methods*. 2009; 6:451–457. [PubMed: 19412169]
43. Stamatakis AM, Stuber GD. Activation of lateral habenula inputs to the ventral midbrain promotes behavioral avoidance. *Nat. Neurosci.* 2012; 15:1105–1107. [PubMed: 22729176]
44. Hagan MM, et al. Long-term orexigenic effects of AgRP-(83–132) involve mechanisms other than melanocortin receptor blockade. *Am. J. Physiol. Regul. Integr. Comp. Physiol.* 2000; 279:R47–52. [PubMed: 10896863]

45. Krashes MJ, Shah BP, Koda S, Lowell BB. Rapid versus Delayed Stimulation of Feeding by the Endogenously Released AgRP Neuron Mediators GABA, NPY, and AgRP. *Cell Metab.* 2013; 18:588–595. [PubMed: 24093681]
46. Avants BB, Epstein CL, Grossman M, Gee JC. Symmetric diffeomorphic image registration with cross-correlation: evaluating automated labeling of elderly and neurodegenerative brain. *Medical image analysis.* 2008; 12:26–41. [PubMed: 17659998]
47. Mukamel EA, Nimmerjahn A, Schnitzer MJ. Automated analysis of cellular signals from large-scale calcium imaging data. *Neuron.* 2009; 63:747–760. [PubMed: 19778505]

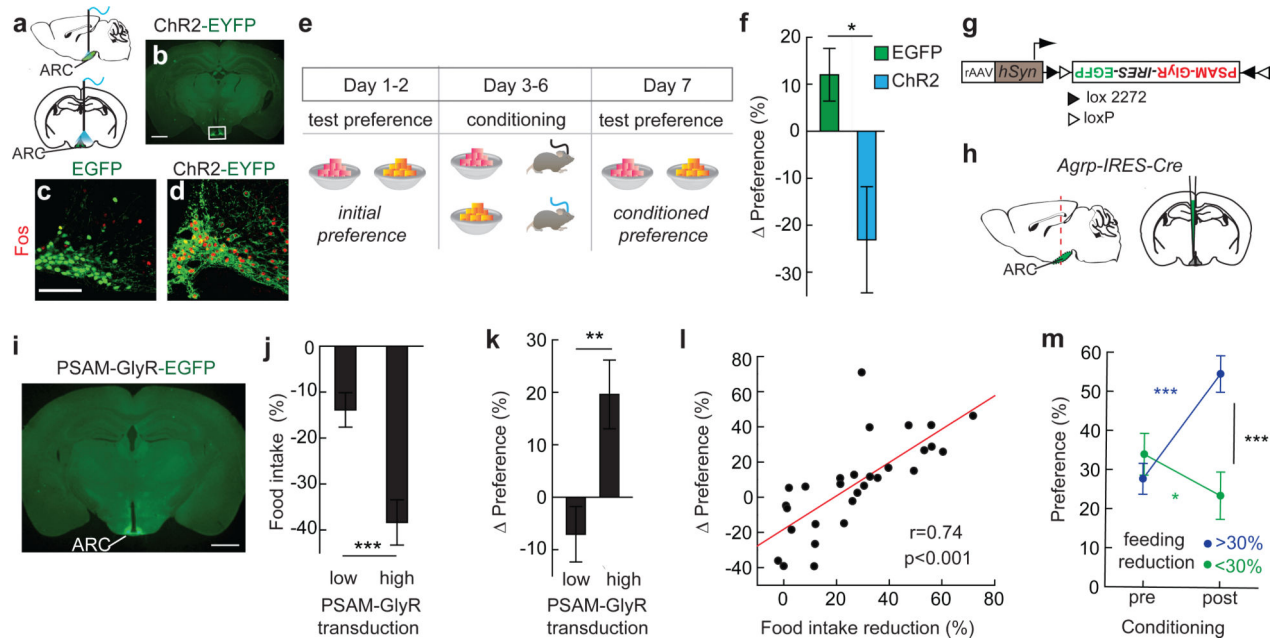


### Figure 1. AGRP neurons condition flavour preference

**a**, Optical fibre position over the arcuate nucleus (ARC). **b**, ChR2-EYFP in AGRP neurons (box). Scale, 1 mm. **c,d**, Fos immunofluorescence following photostimulation in AGRP<sup>EGFP</sup> (**c**) or AGRP<sup>ChR2</sup> (**d**) mice. Scale, 100  $\mu$ m. **e**, Experimental design of conditioned flavour preference assay in AL-fed AGRP<sup>ChR2</sup> or AGRP<sup>EGFP</sup> mice. **f**, Change in preference for flavour paired with light in AGRP<sup>EGFP</sup> and AGRP<sup>ChR2</sup> mice (EGFP, n=6; ChR2, n=8). **g,h** Injection of rAAV (**g**) for Cre-dependent expression of PSAM<sup>L141F</sup>-GlyR-*IRES*-EGFP in (**h**) AGRP neurons. **i**, Image of virally transduced AGRP neurons showing PSAM<sup>L141F</sup>-GlyR-*IRES*-EGFP expression. Scale, 1 mm. **j**, Chow food intake reduction for food-restricted (FR) mice treated with PSEM<sup>89S</sup> grouped by transgene transduction efficiency (low:<50%, n=13; high:>50%, n=16). **k**, Change in preference for flavour paired with PSEM<sup>89S</sup> injection in FR AGRP<sup>PSAM-GlyR</sup> mice. **l**, Change in preference correlates with reduction of chow food intake (n=29 mice). **m**, Flavour preference pre- and post-conditioning for mice grouped by *post hoc* food intake reduction test. \*p<0.05, \*\*p<0.01, \*\*\*p<0.001. Values are means  $\pm$  s.e.m. Statistical analysis in Extended Data Table 1.

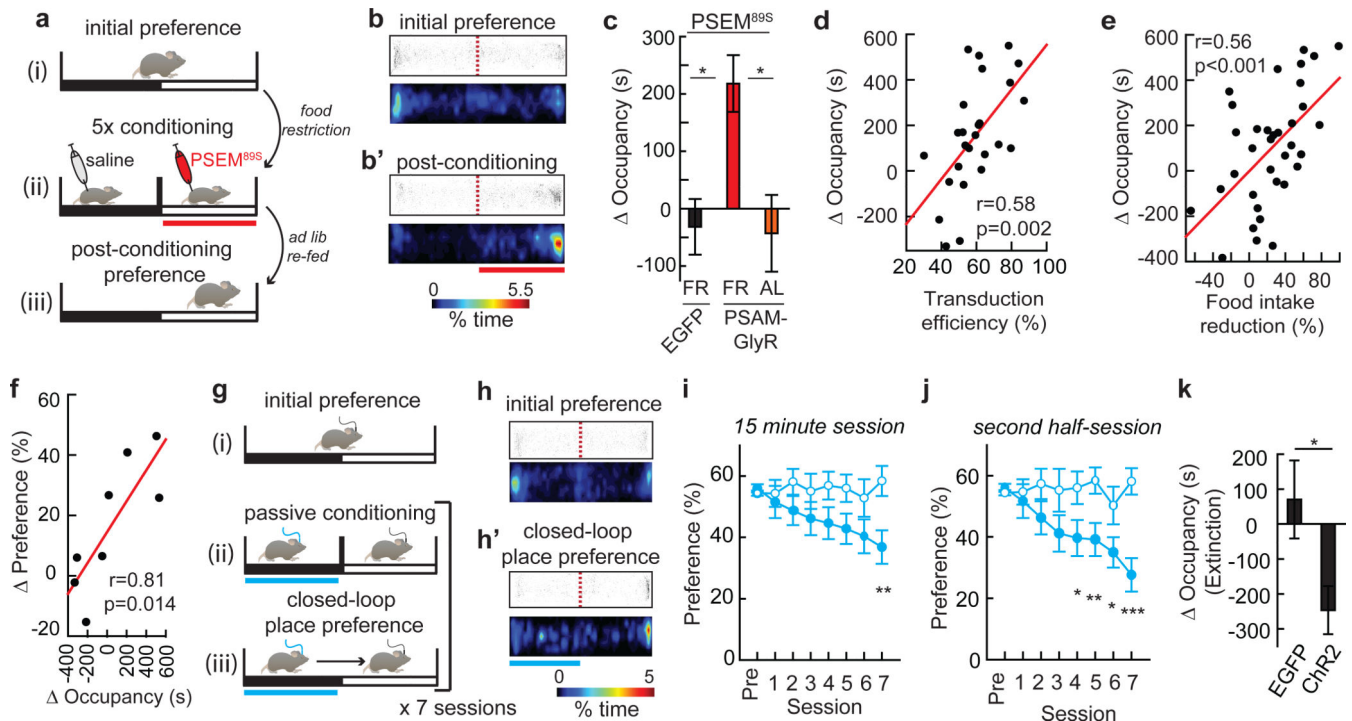


**Figure 2. AGRP neurons condition place preference**

**a**, Experimental design of place preference conditioning with chemogenetic silencing. Red bar: chemogenetic silencing side. **b,b'**, For a FR AGRP<sup>PSAM-GlyR</sup> mouse, scatter plot of position and a heat map showing percent occupancy time. **c**, Change in occupancy time for AGRP<sup>EGFP</sup> mice (n=13), FR AGRP<sup>PSAM-GlyR</sup> mice (n=20) or AL AGRP<sup>PSAM-GlyR</sup> mice (n=9) with >50% PSAM<sup>L141F</sup>-GlyR transduction efficiency after conditioning with PSEM<sup>89S</sup> injections. **d,e**, Change in occupancy time for side paired with PSEM<sup>89S</sup> is correlated with **(d)** PSAM<sup>L141F</sup>-GlyR transduction efficiency (n=26 mice) and **(e)** chow food intake reduction for mice treated with PSEM<sup>89S</sup> (n=35 mice). **f**, Preference shift is correlated for place and flavour conditioning. **g**, Experimental design for place conditioning during optogenetic activation. Blue bar: photostimulated side. **h,h'**, For an AGRP<sup>Chr2</sup> mouse, scatter plots of position and heat maps showing percent occupancy time. **i,j**, Percent occupancy time on photostimulated side for AGRP<sup>EGFP</sup> (open circles, n=12) or AGRP<sup>Chr2</sup> (filled circles, n=12) mice during **(i)** 15-min conditioning sessions (2-way repeated measures ANOVA, group:  $F_{(1,154)}=3.0$ ,  $p=0.097$ ; session:  $F_{(7,154)}=2.3$ ,  $p=0.029$ ; interaction:  $F_{(7,154)}=3.3$ ,  $p=0.003$ ) and **(j)** second half of each 15-min session (group:  $F_{(1,154)}=6.4$ ,  $p=0.019$ ; session:  $F_{(7,154)}=3.2$ ,  $p=0.004$ ; interaction:  $F_{(7,154)}=3.8$ ,  $p<0.001$ ). **k**, Change in occupancy time on the previously photostimulated side for AGRP<sup>EGFP</sup> (open circles, n=12) or AGRP<sup>Chr2</sup> (filled circles, n=12) mice during 1800-s extinction session. \* $p<0.05$ , \*\* $p<0.01$ , \*\*\* $p<0.001$ . Values are means  $\pm$  s.e.m. Statistical analysis in Extended Data Table 1.

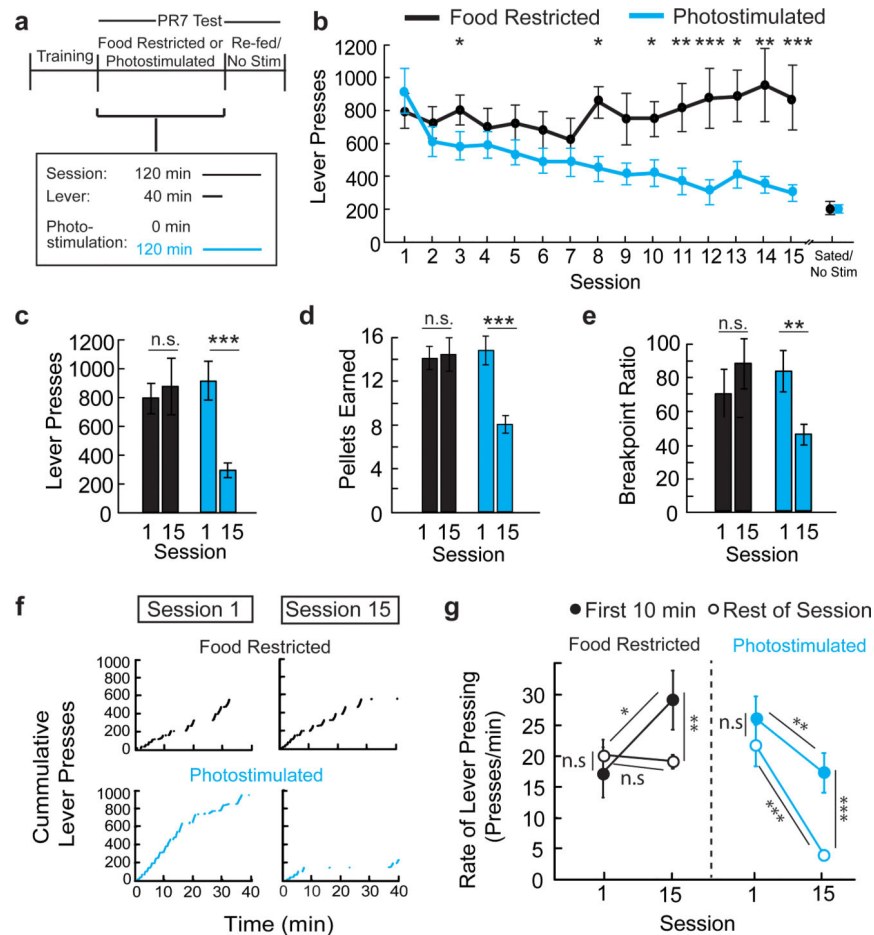


### Figure 3. Modulation of instrumental responding for food

**a**, Experimental design. AGRP<sup>ChR2</sup> mice were trained to lever press for food pellets. PR7 reinforcement testing was performed over 15 sessions on two groups: food-restricted (black, n=11) or *ad libitum* fed AGRP neuron photostimulated (cyan, n=11). During test sessions (120 min), levers were available for the first 40 minutes. The AGRP neuron photostimulated group received intracranial light pulses for the entire 120-min session. **b**, Lever presses in each session during PR7 reinforcement. **c-e**, Lever presses (**c**), pellets earned (**d**), and breakpoint ratio (**e**) from first (1) and last (15) PR7 reinforcement test sessions. **f**, Representative traces of cumulative lever pressing during first (1) and last (15) sessions. **g**, Rate of lever pressing during first 10 minutes of session (low effort reinforcement, filled circles) and rest of session (high-effort reinforcement, open circles) on first (1) and last (15) PR7 session. n.s. p>0.05, \*p<0.05, \*\*p<0.01, \*\*\*p<0.001. Values are means  $\pm$  s.e.m. Statistical analysis in Extended Data Table 1.

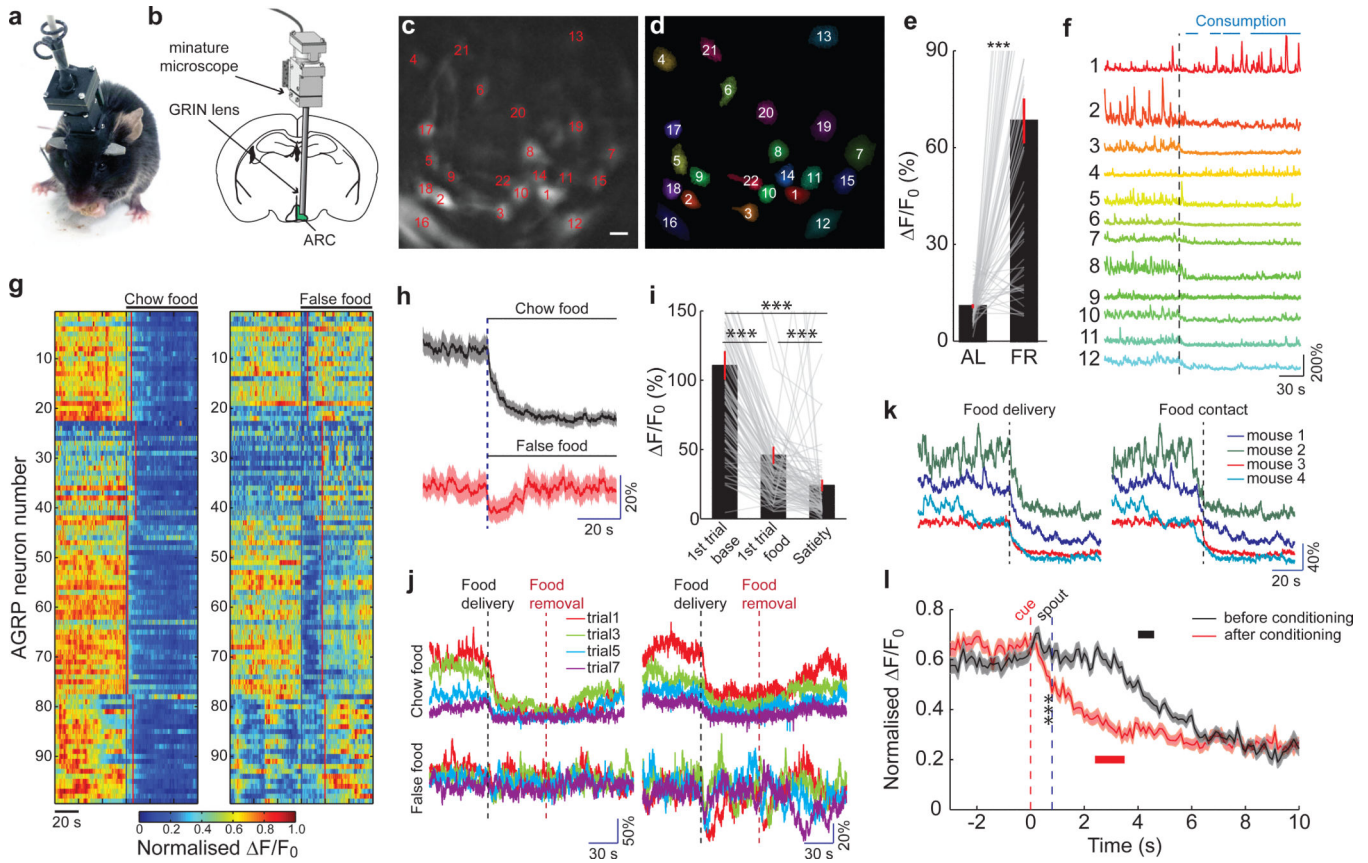


**Figure 4. Food rapidly reduces AGRP neuron activity**  
**a,b** Configuration for deep-brain calcium imaging from AGRP neurons in freely-moving mice. **c,d**, Image of AGRP<sup>GCaMP6f</sup> neurons (**c**) by deep-brain calcium imaging and their ROI spatial filters (**d**) for image analysis. Scale bar, 15  $\mu$ m. **e**, Change in baseline GCaMP6 fluorescence for neurons in mice under AL-fed and FR conditions (61 neurons, 4 mice). **f**, From FR mice, GCaMP6f fluorescence traces from subset of individual neurons in (**c,d**) during chow pellet food consumption. Black line, food delivery. Blue bars, food consumption. **g**, Normalised Ca<sup>2+</sup> responses of AGRP neurons (99 neurons, 4 FR mice) during exposure to a chow food pellet (left) and a false food pellet (right). Black lines, chow/false food delivery. Red lines, first contact with chow/false food. **h**, Mean calcium responses to chow food and false food aligned to delivery time (99 neurons, 4 FR mice). Shading: s.e.m. **i**, Change in normalised GCaMP6 fluorescence comparing initial baseline activity, first food exposure, and after consuming to satiety (110 neurons, 4 FR mice). **j**, GCaMP6f fluorescence traces from 2 example neurons (2 mice) during short trials of food (top) and false food (bottom) delivery. **k**, Mean GCaMP6 fluorescence responses from individual mice to chow food exposure aligned with food delivery (left) and food contact (right). **l**, Mean GCaMP6 fluorescence responses before (black) and after (red) cued Pavlovian trace conditioning (before: 60 neurons, after: 65 neurons, 3 mice). Black and red bars, range for first lick of liquid food. Shading: s.e.m. \*\*\* $p < 0.001$ . Values are means  $\pm$  s.e.m.

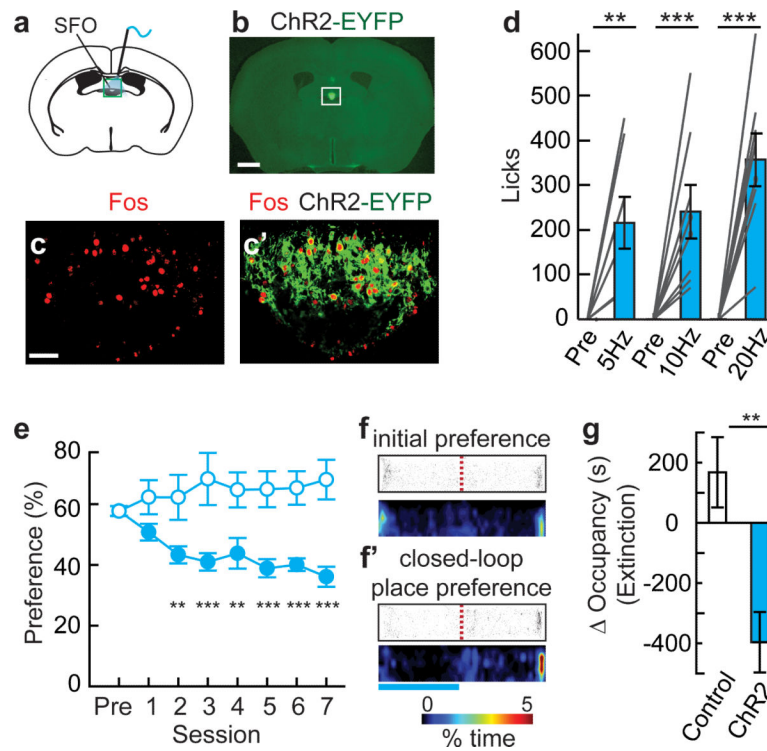


### Figure 5. Virtual dehydration state is avoided

**a**, Optical fibre position over SFO (box). **b**, Expression of ChR2-EYFP in SFO<sup>NOS1</sup> neurons. Scale, 1 mm. **c,c'**, Fos immunofluorescence following photostimulation in SFO<sup>NOS1-ChR2</sup> mice. Scale, 100  $\mu$ m. **d**, Water consumption by SFO<sup>NOS1-ChR2</sup> mice either before or during photostimulation (1 h) at different frequencies (n=8). **e,f**, Closed-loop place preference for SFO<sup>NOS1-ChR2</sup> mice (filled circles, n=12) and untransfected controls (open circles, n=6) as in Fig. 3e. Blue bar: photostimulated side. (group:  $F_{(1,112)}=26.2$ ,  $p<0.001$ ; session:  $F_{(7,112)}=0.74$ ,  $p=0.64$ ; interaction:  $F_{(7,112)}=4.25$ ,  $p<0.001$ ). **g**, Change in occupancy time during an extinction session for the photostimulated side for SFO<sup>NOS1-ChR2</sup> mice (n=12) and untransfected controls (n=6). \* $p<0.05$ , \*\* $p<0.01$ , \*\*\* $p<0.001$ . Values are means  $\pm$  s.e.m.